Electronic Supplementary Material (ESI) for Dalton Transactions.

The Synthesis and Structures of 1,1'-Bis(sulfonyl)ferrocene Derivatives

Kullapa Chanawanno,[a] Cole Holstrom,[b] Laura A. Crandall,[c] Henry Dodge,[d] Victor N. Nemykin,[b] Richard S. Herrick[d] and Christopher J. Ziegler*[c]

a. Department of Chemistry, Faculty of Science, Chiang Mai University, Chiang Mai 50200 (Thailand).

b. Department of Chemistry & Biochemistry University of Minnesota – Duluth 1039 University Drive, Duluth, MN 55812 (USA).

c. Department of Chemistry, University of Akron, Akron, Ohio 44312-3601 (USA). Email: ziegler@uakron.edu

d. Department of Chemistry, College of the Holy Cross, 1 College St, Worcester, MA 01610 (USA).

Supplementary Information

Table of Contents

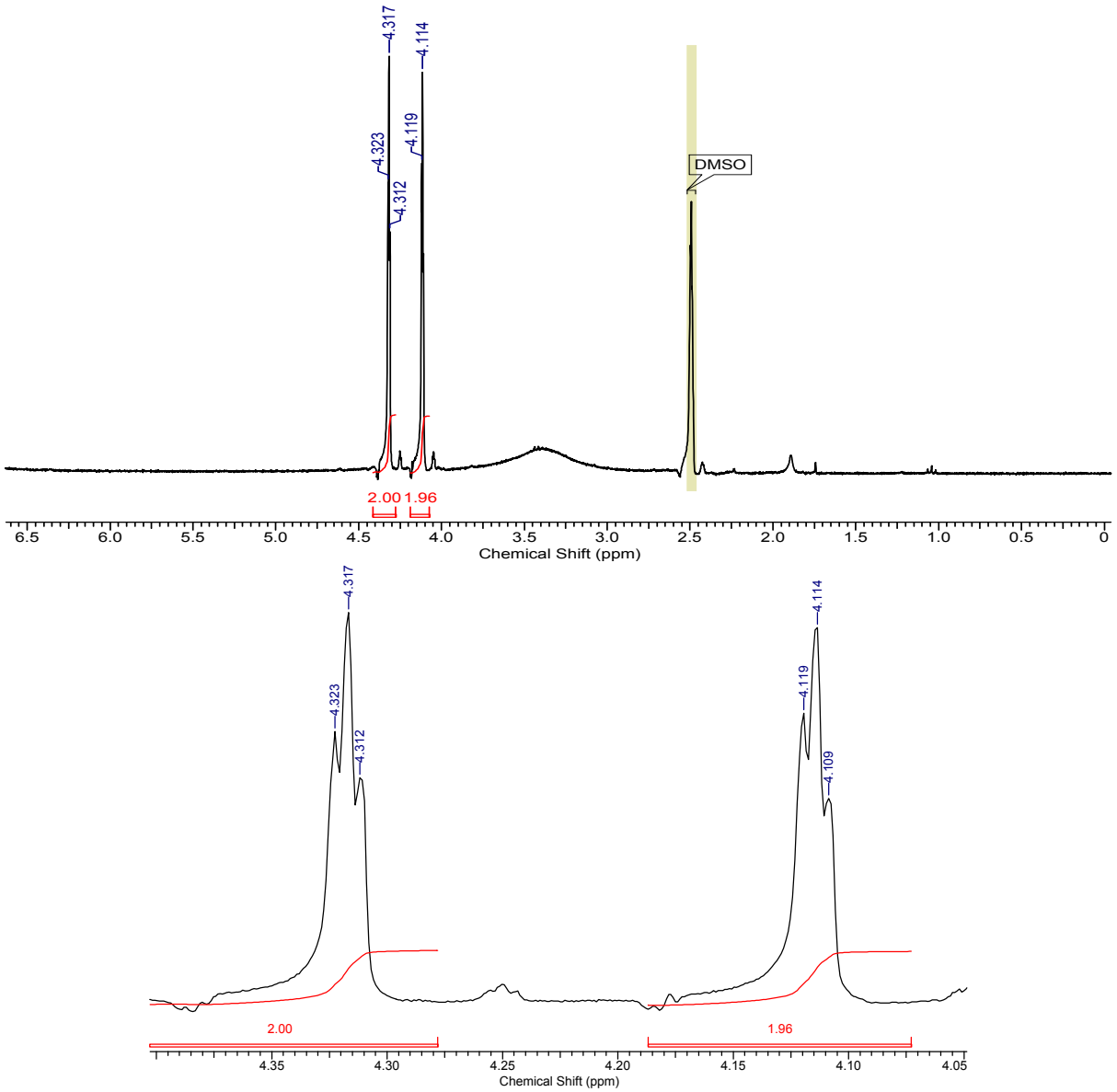

Figure S1 ^{1}H-NMR of **2** (300 MHz, DMSO-d_6)

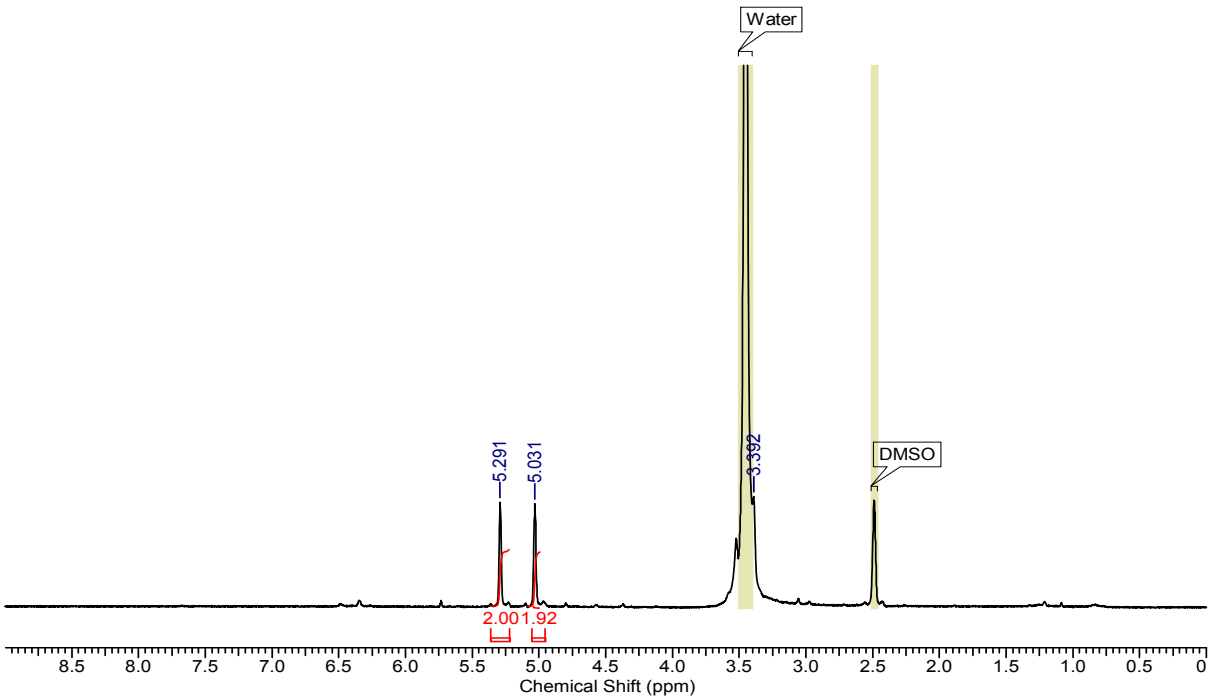

Figure S2 ^{1}H-NMR of **3** (300 MHz, DMSO-d_6)

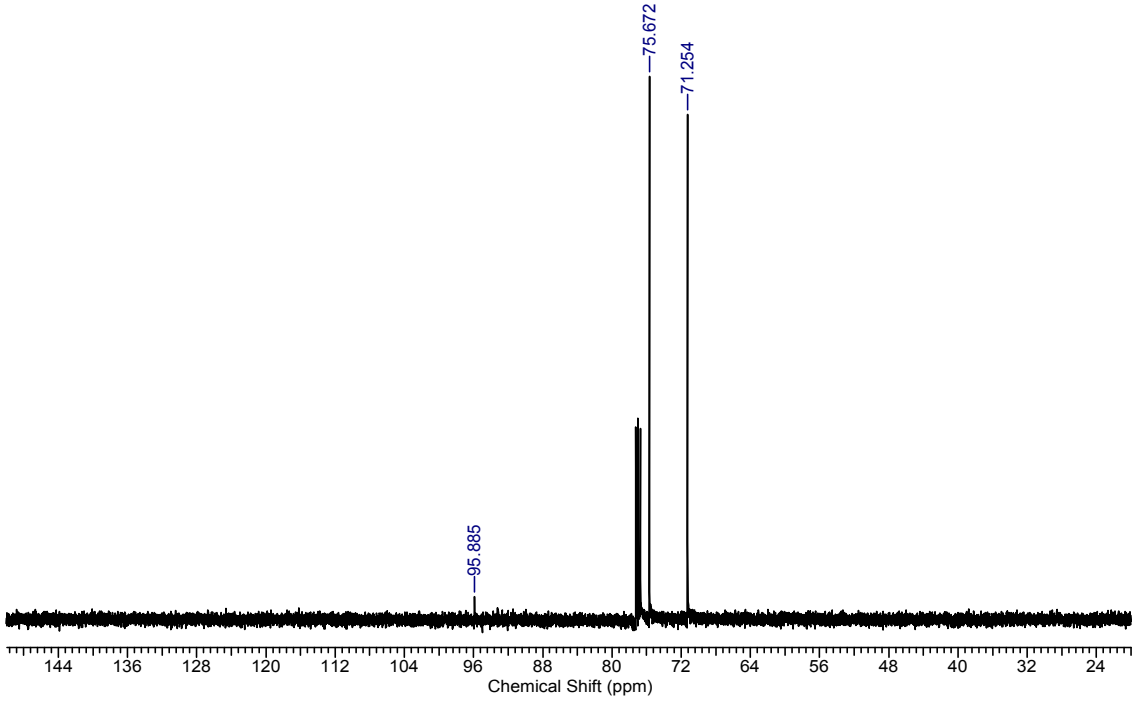

Figure S3 ^{13}C-NMR of **3** (500 MHz, $CDCl_3$)

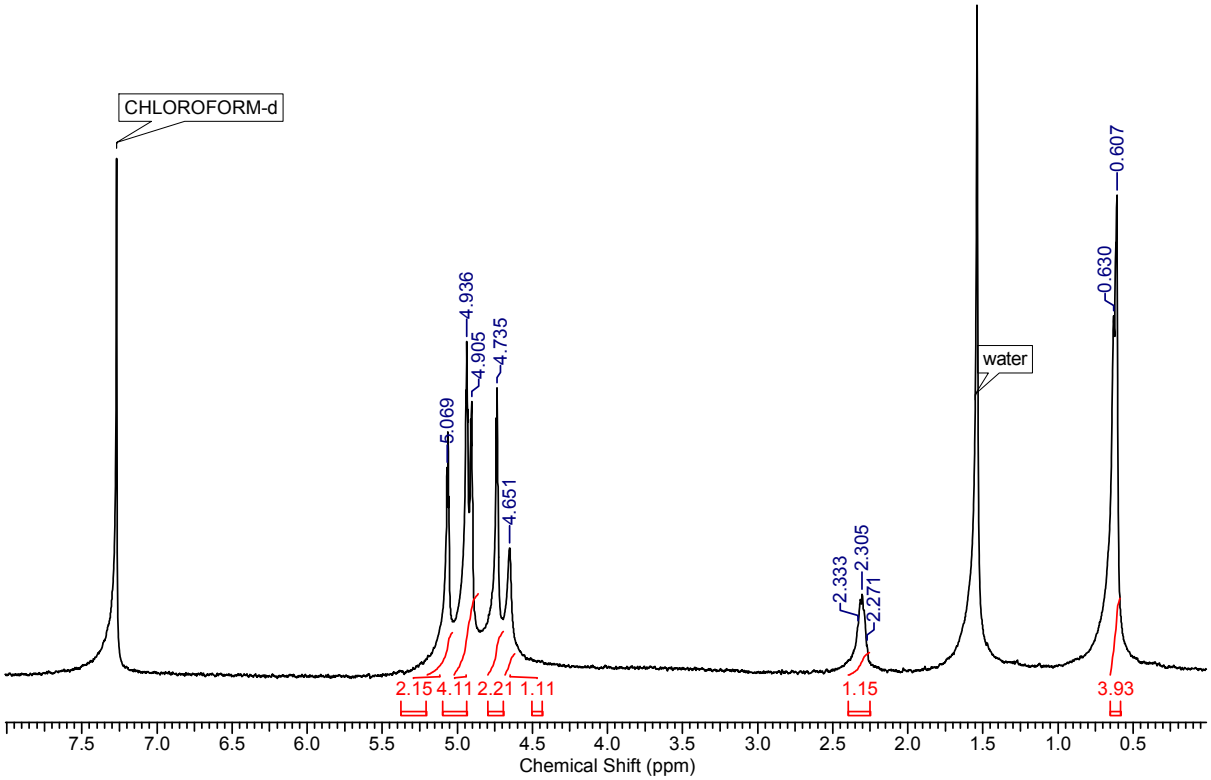

Figure S4 ^{1}H-NMR of **4** (300 MHz, $CDCl_3$)

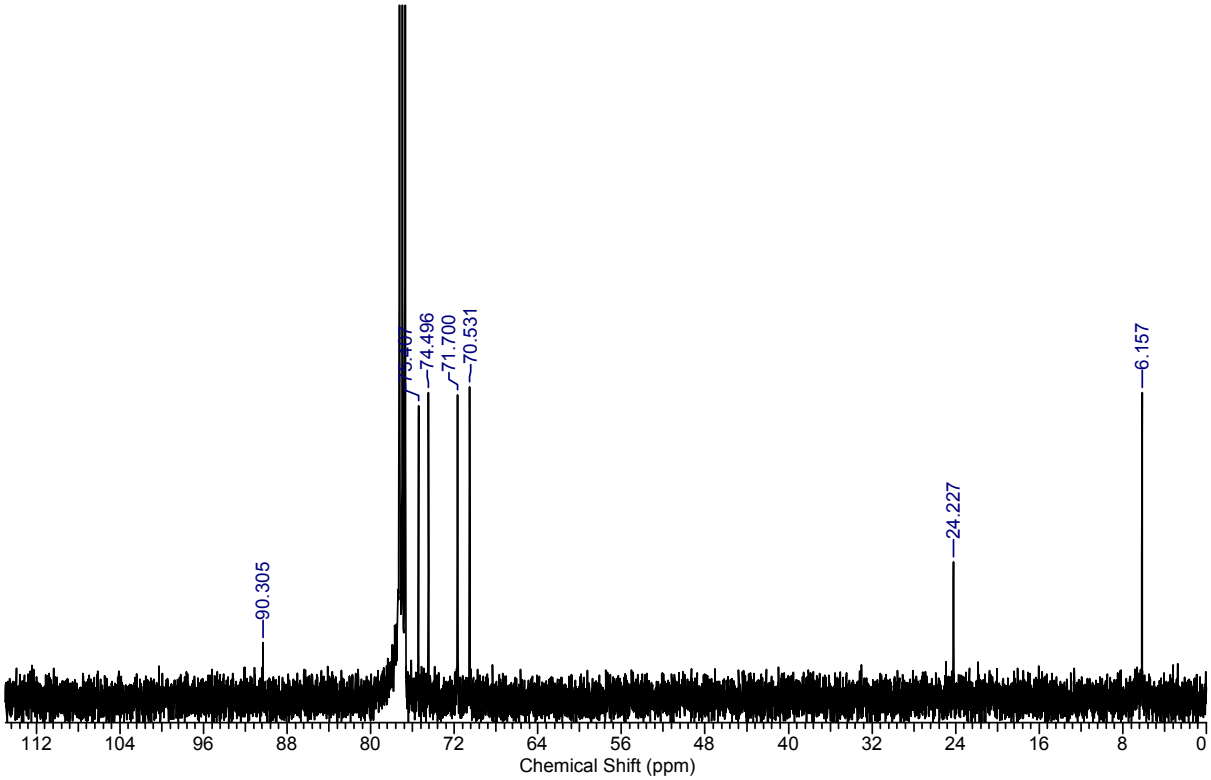

Figure S5 ^{13}C-NMR of **4** (500 MHz, $CDCl_3$)

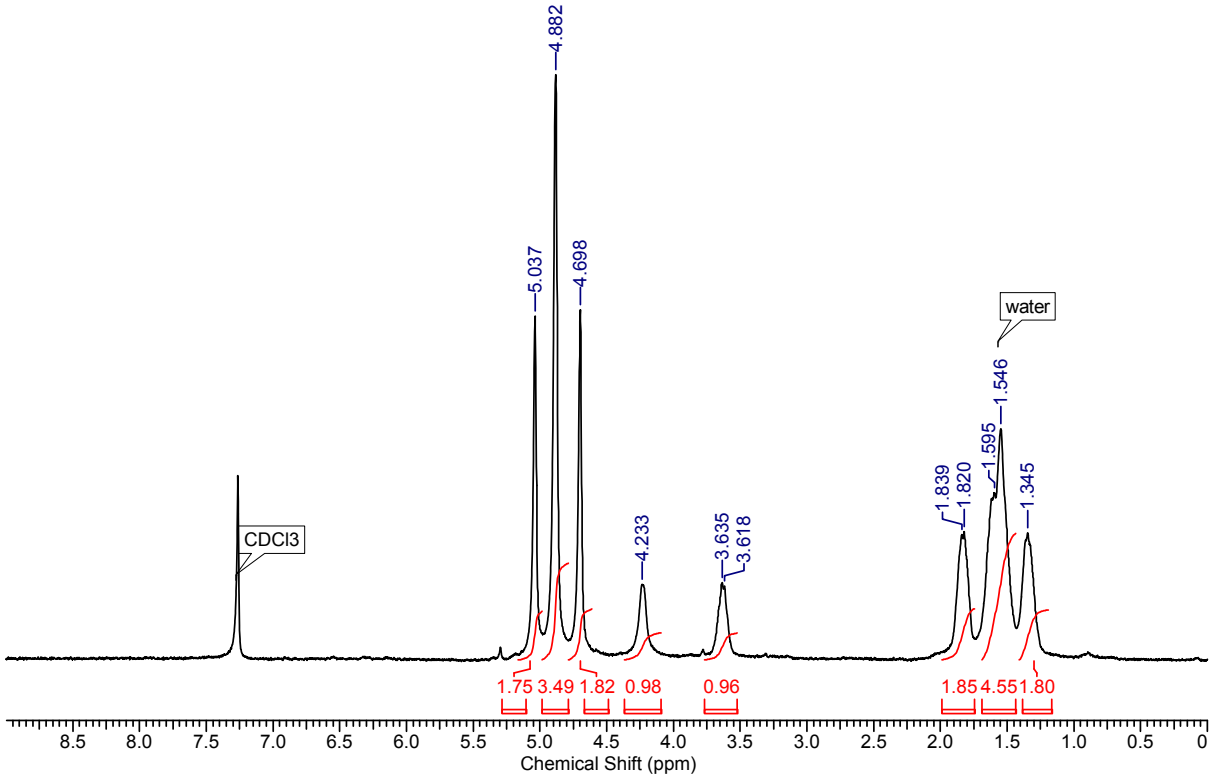

Figure S6 ^{1}H-NMR of **5** (300 MHz, $CDCl_3$)

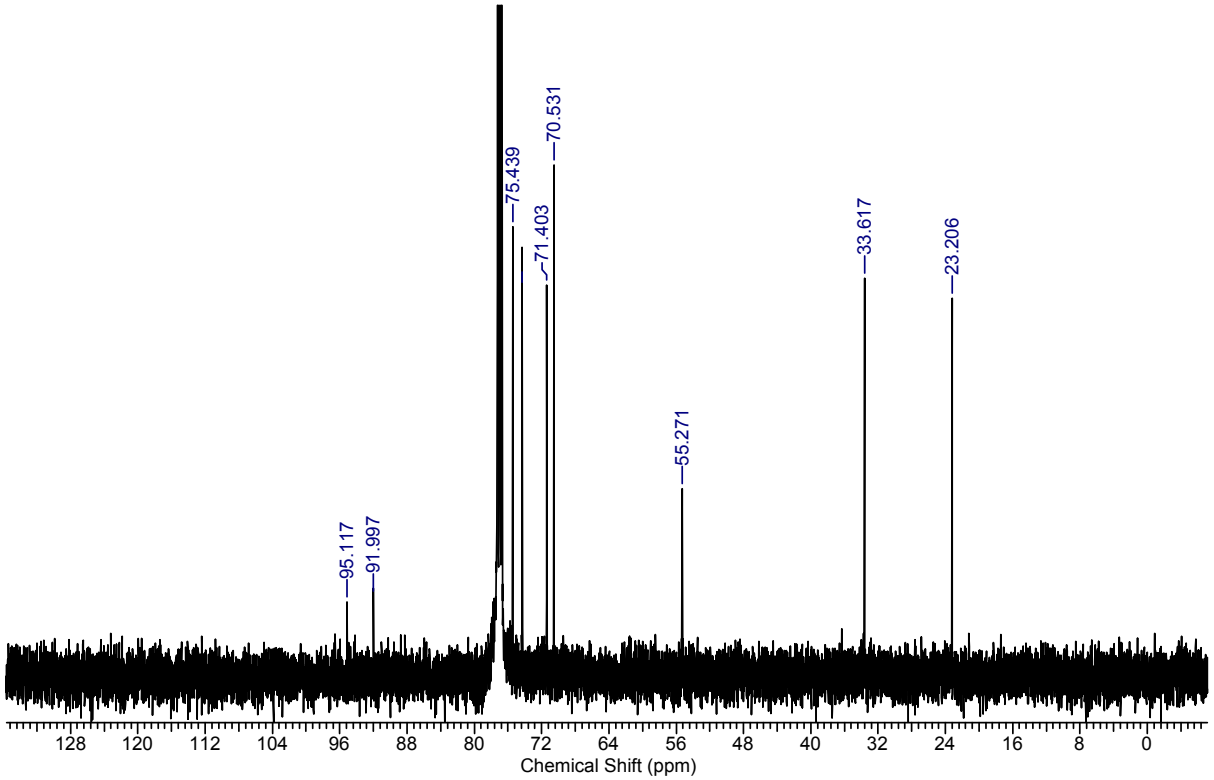

Figure S7 ^{13}C-NMR of **5** (500 MHz, $CDCl_3$)

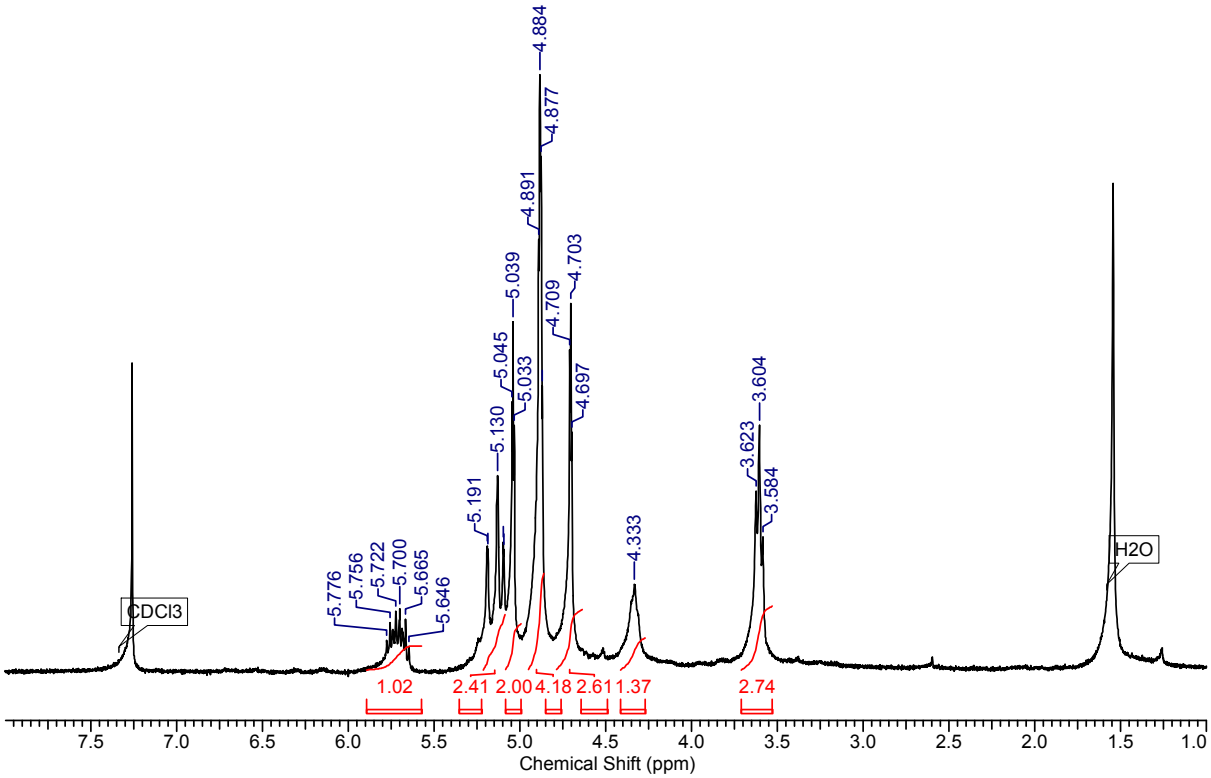

Figure S8 ^{1}H-NMR of **6** (300 MHz, $CDCl_3$)

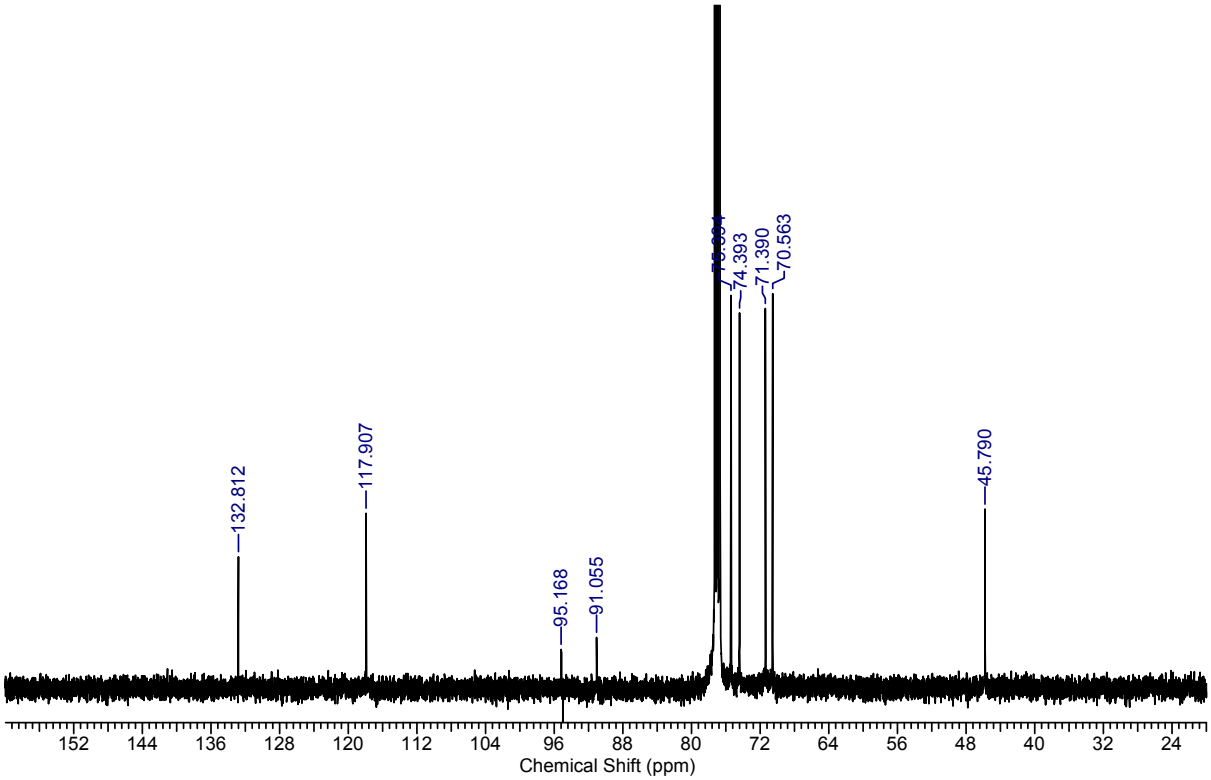

Figure S9 ^{13}C-NMR of **6** (500 MHz, $CDCl_3$)

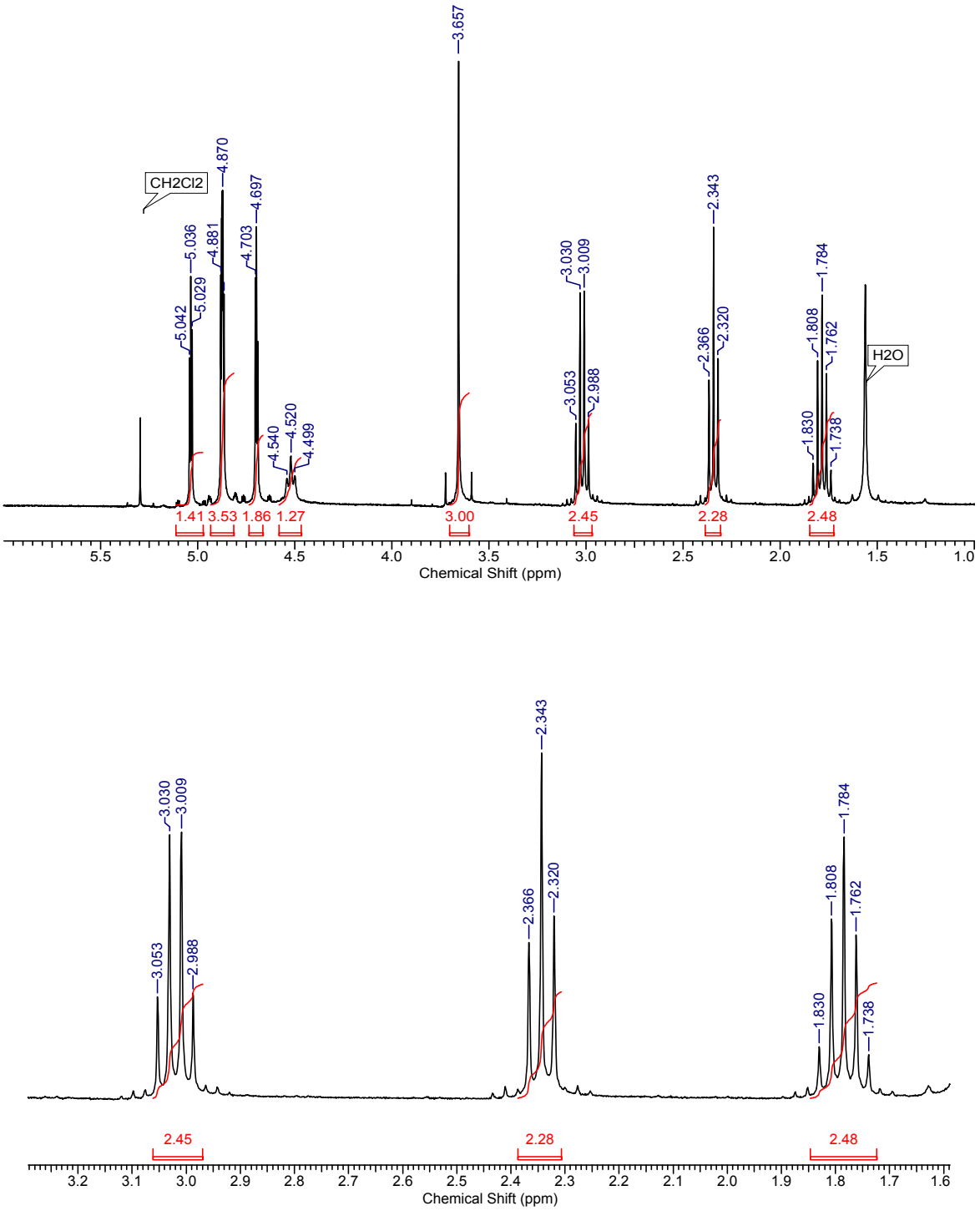

Figure S10 ^{1}H-NMR of **7** (300 MHz, $CDCl_3$)

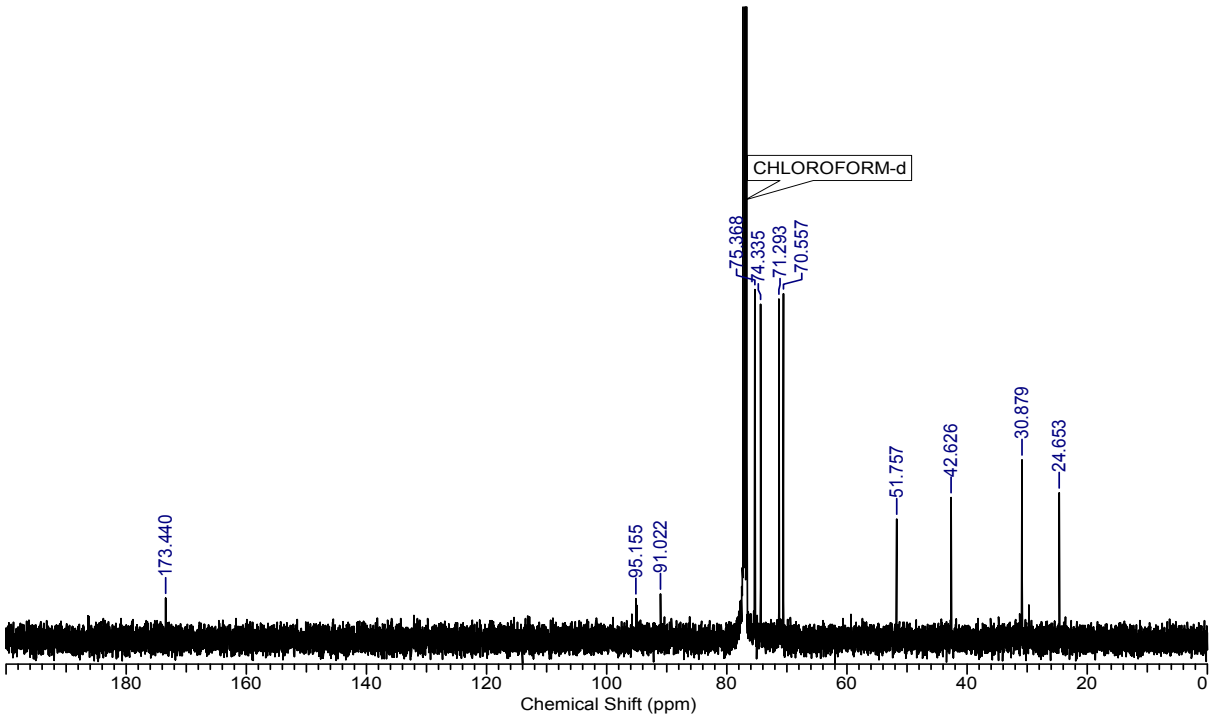

Figure S11 ^{13}C-NMR of **7** (500 MHz, $CDCl_3$)

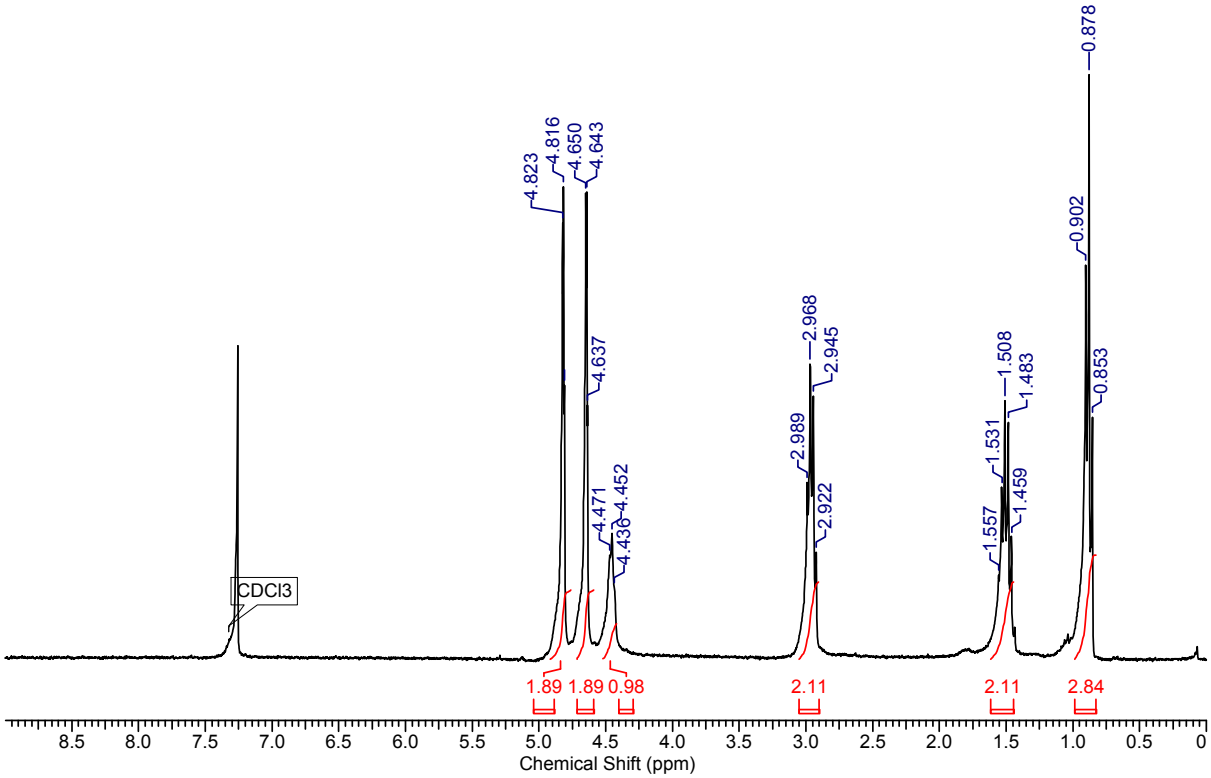

Figure S12 ^{1}H-NMR of **8** (300 MHz, $CDCl_3$)

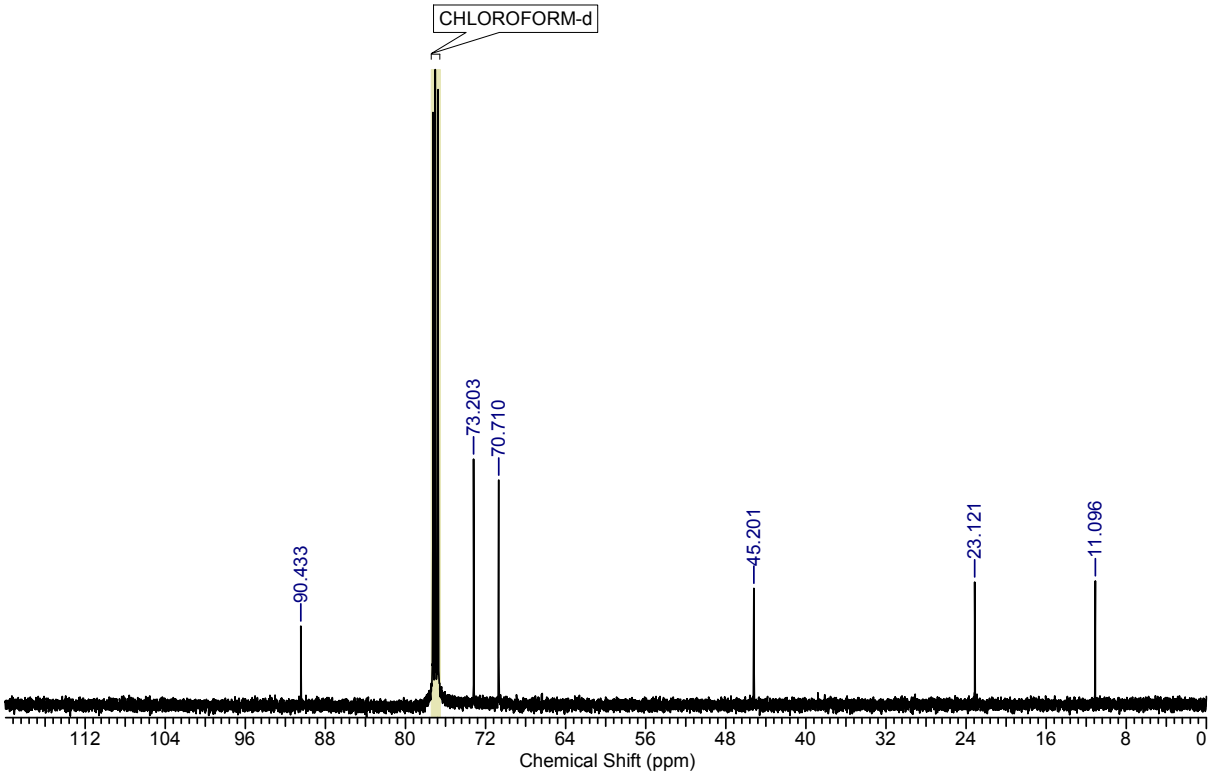

Figure S13 ^{13}C-NMR of **8** (500 MHz, $CDCl_3$)

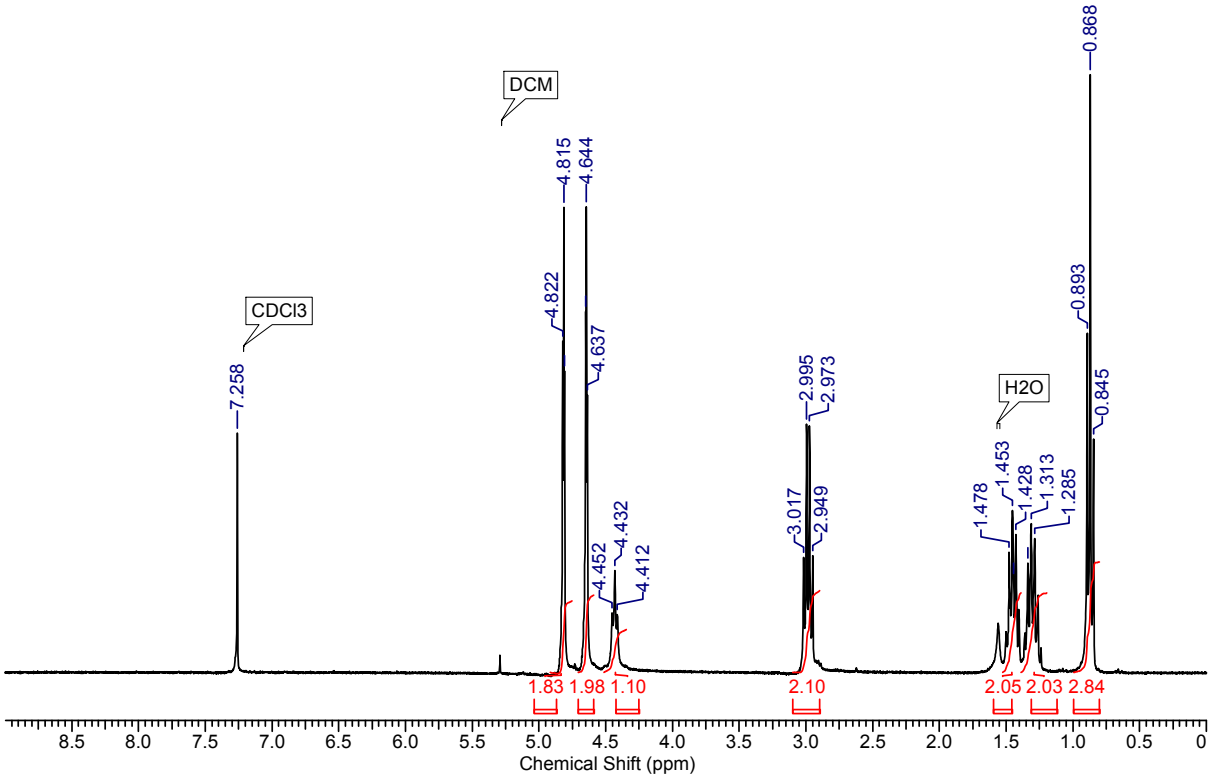

Figure S14 ^{1}H-NMR of **9** (300 MHz, $CDCl_3$)

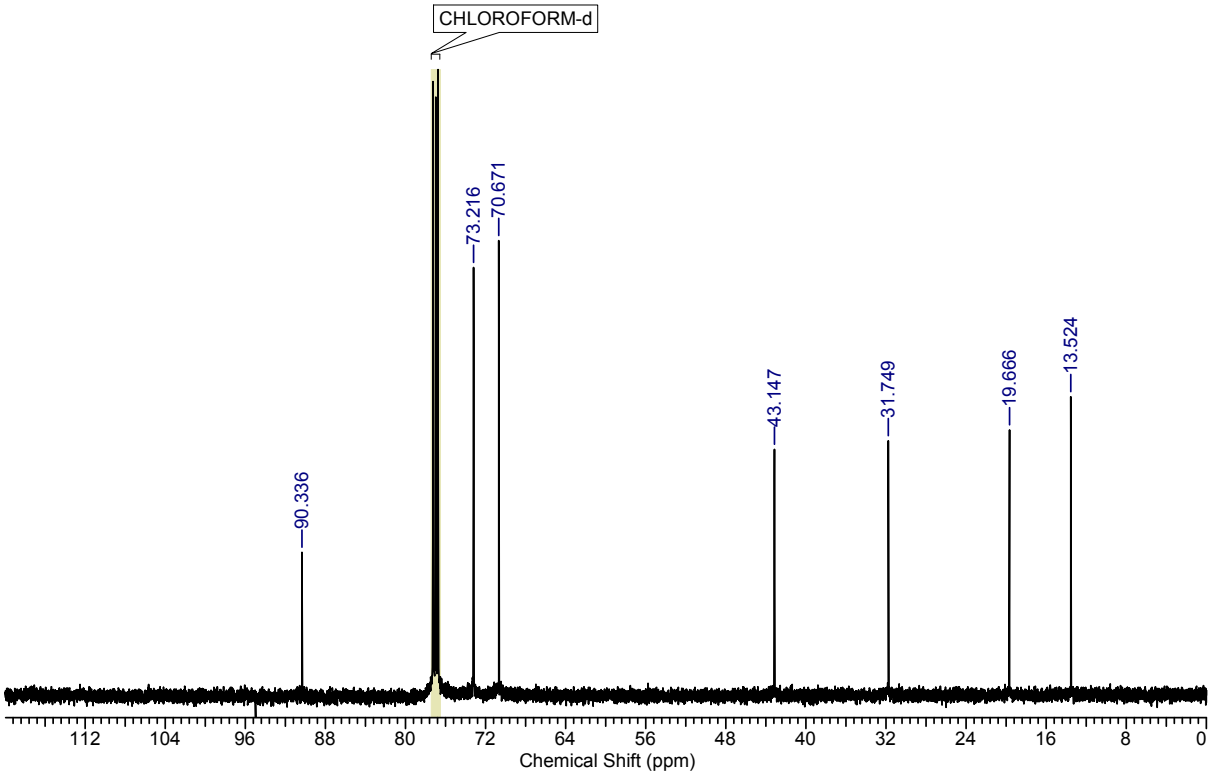

Figure S15 ^{13}C-NMR of **9** (500 MHz, $CDCl_3$)

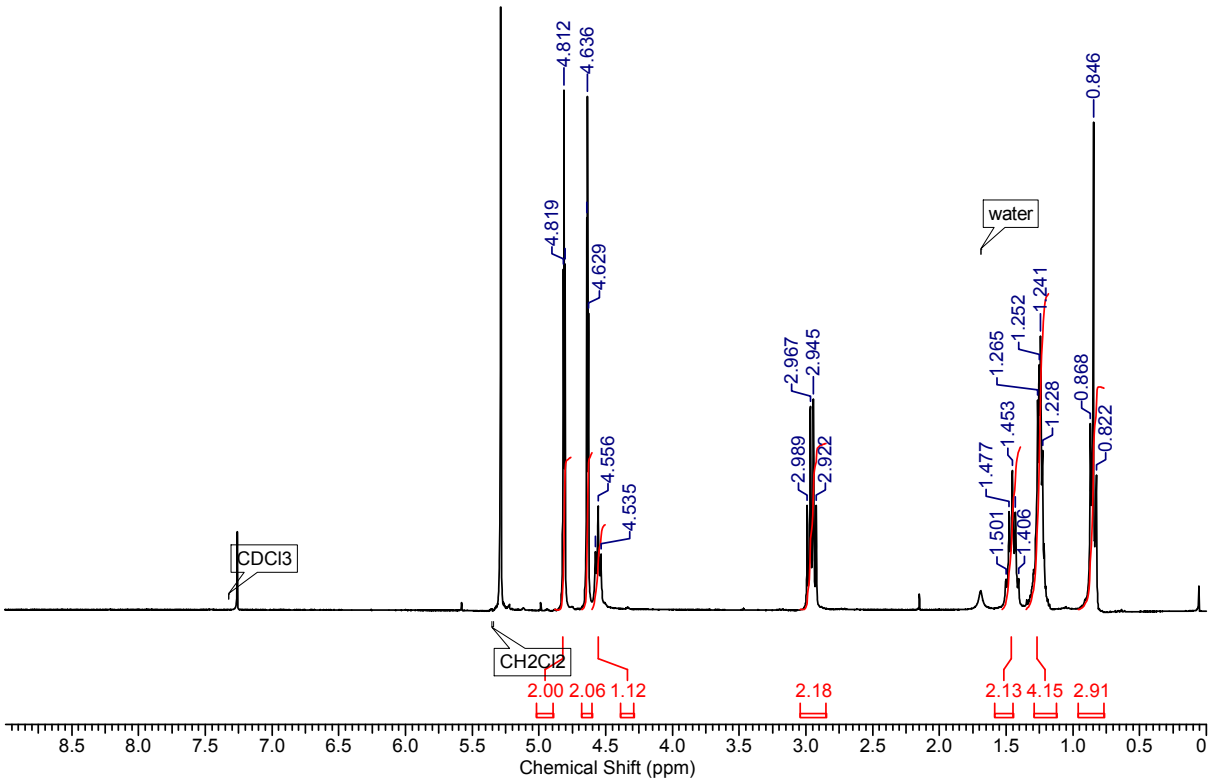

Figure S16 ^{1}H-NMR of **10** (300 MHz, $CDCl_3$)

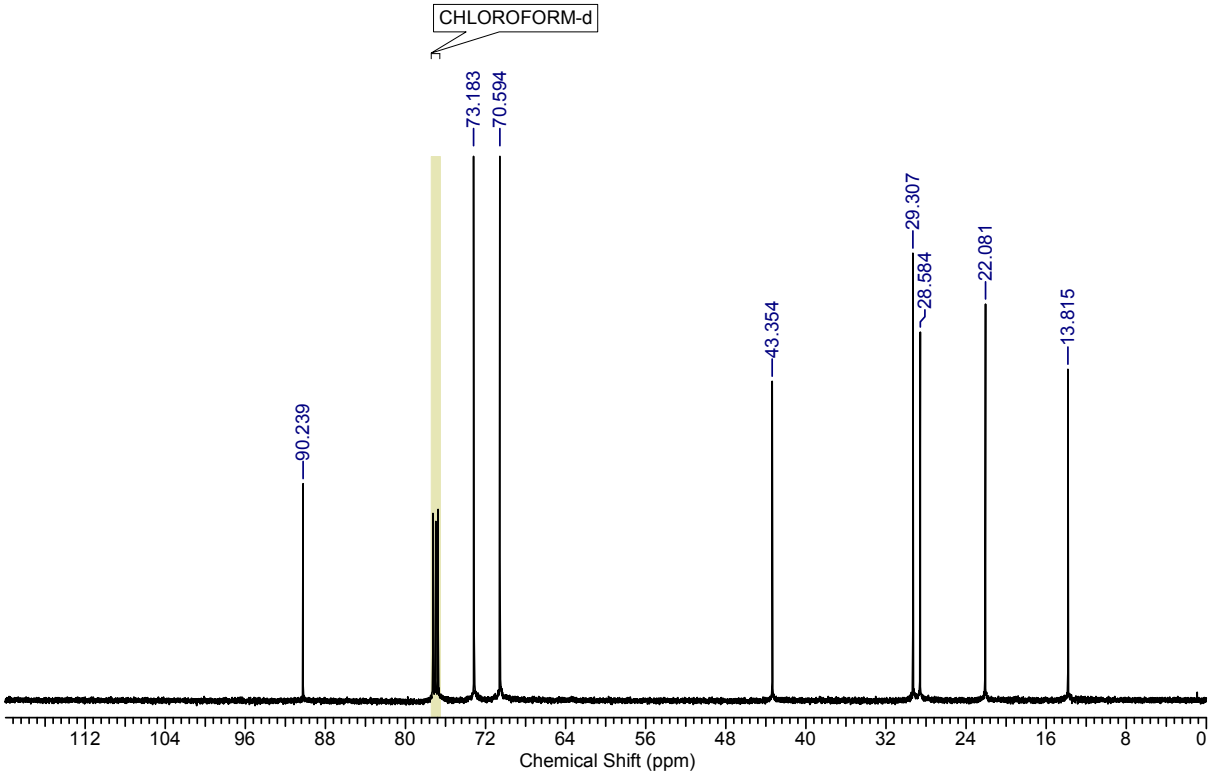

Figure S17 ^{13}C-NMR of **10** (500 MHz, $CDCl_3$)

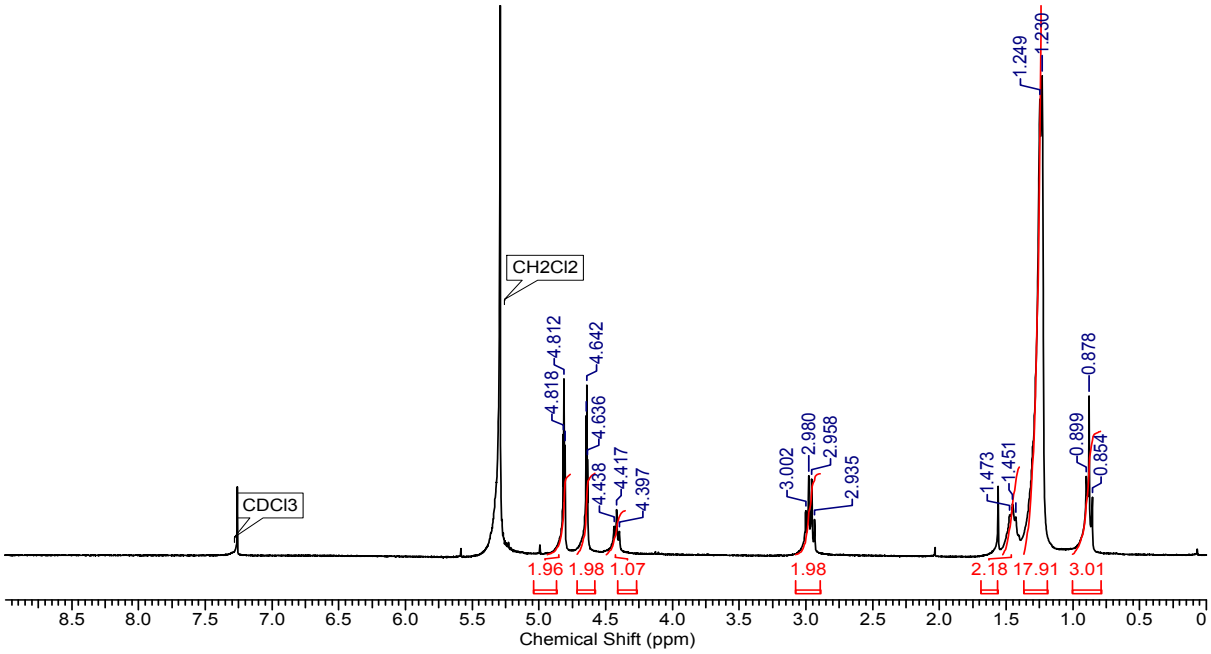

Figure S18 ^{1}H-NMR of **11** (300 MHz, $CDCl_3$)

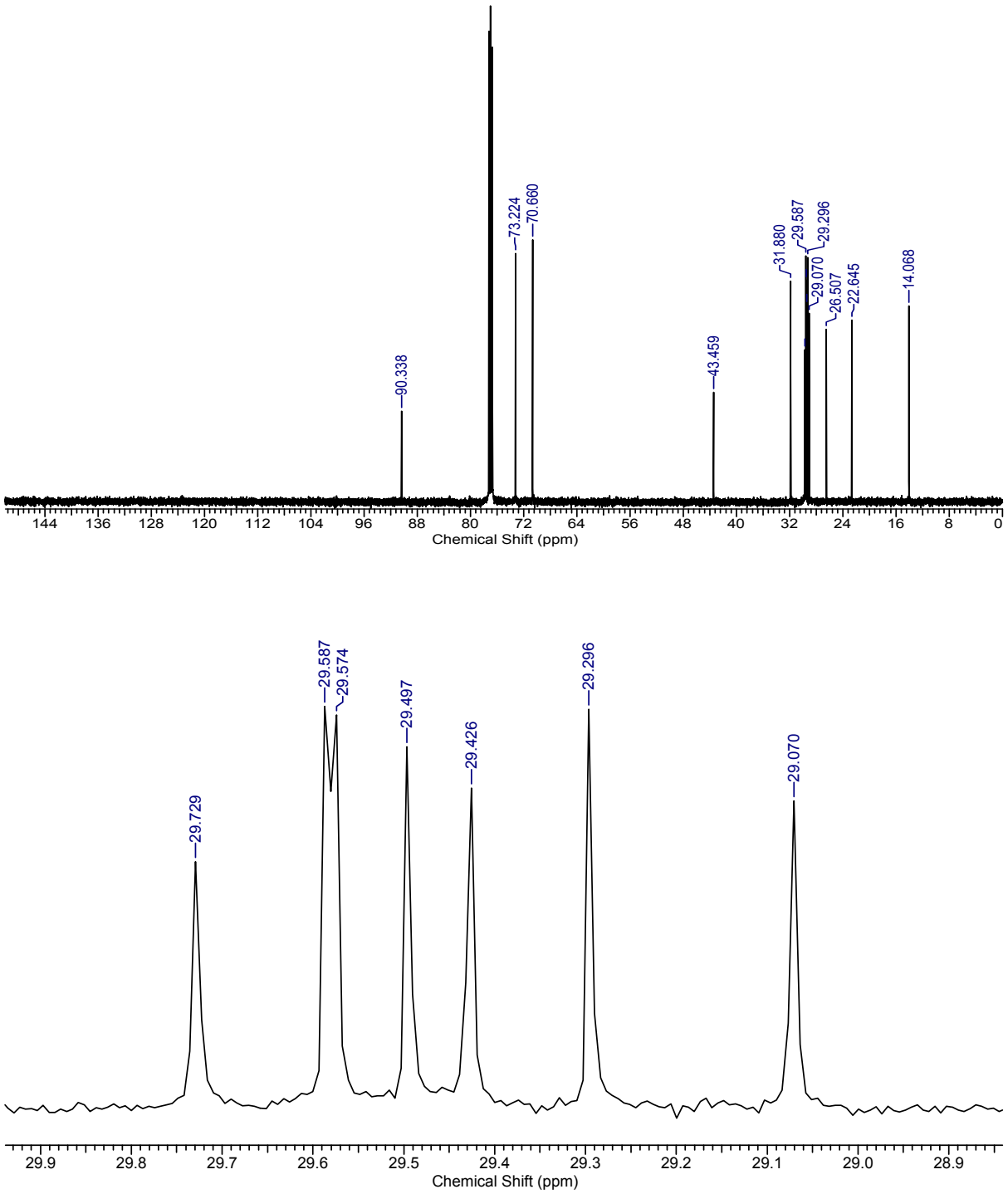

Figure S19 ^{13}C-NMR of **11** (500 MHz, $CDCl_3$)

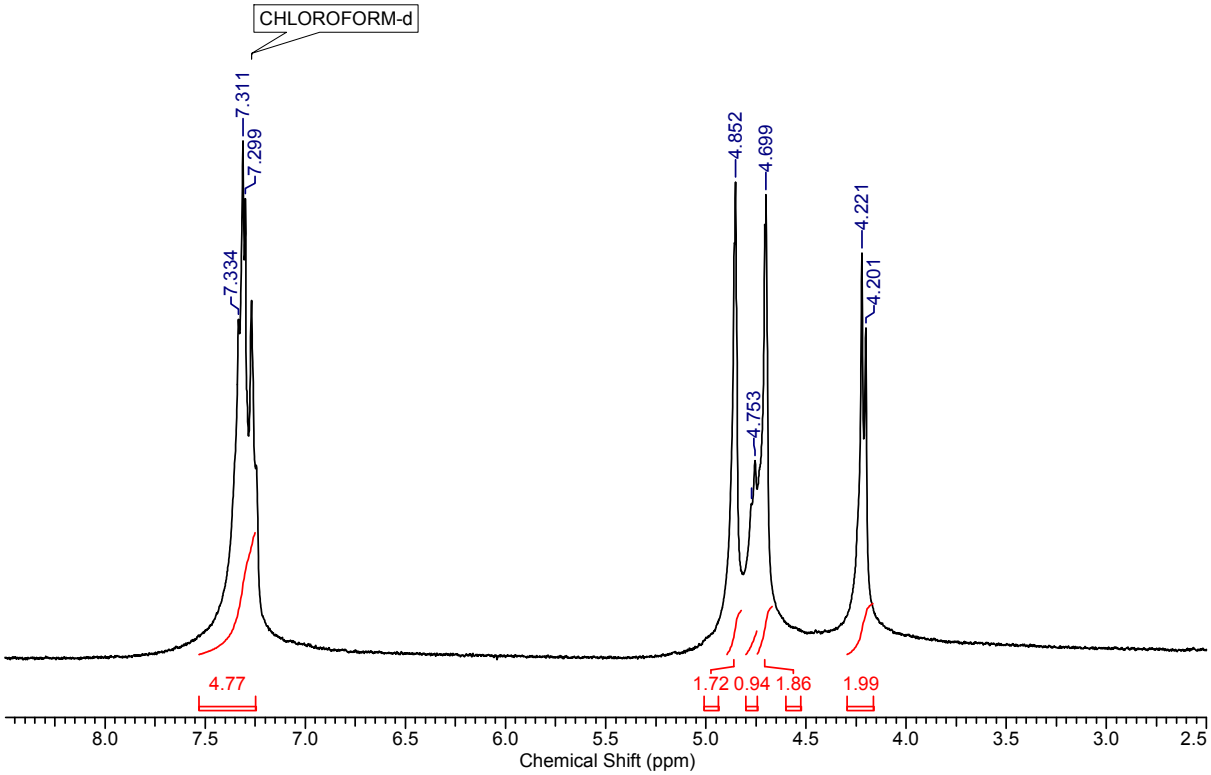

Figure S20 ^{1}H-NMR of **12** (300 MHz, $CDCl_3$)

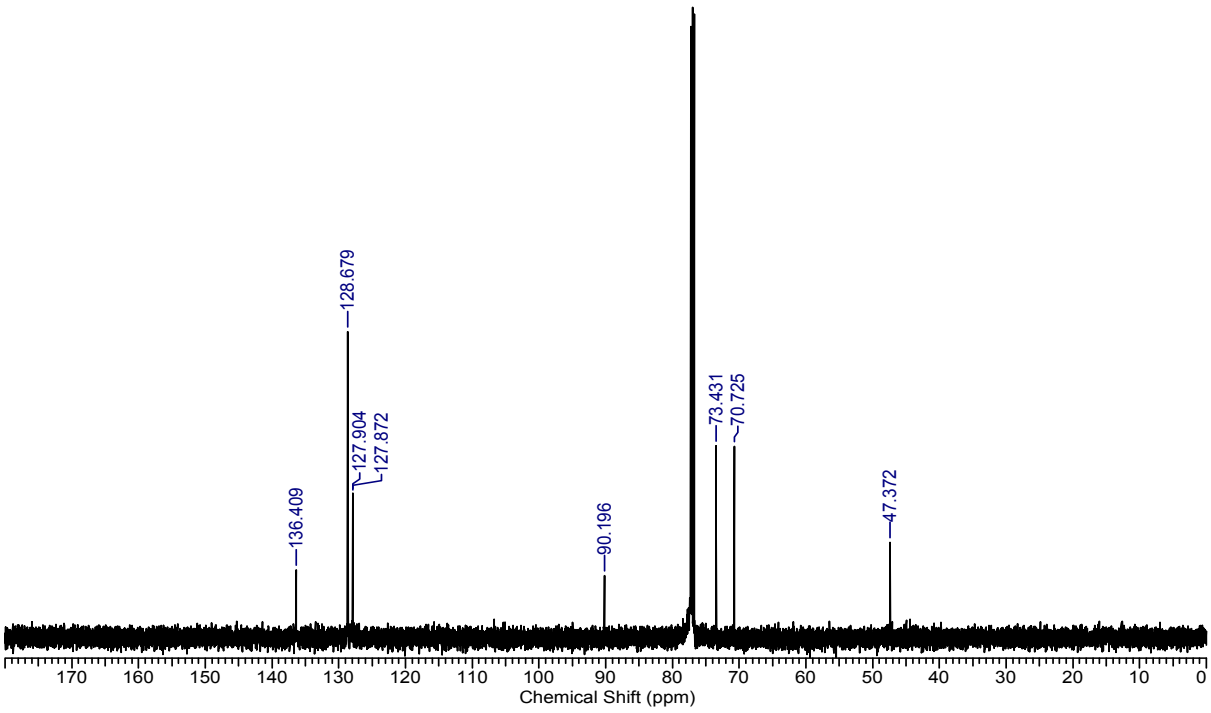

Figure S21 ^{13}C-NMR of **12** (500 MHz, $CDCl_3$)

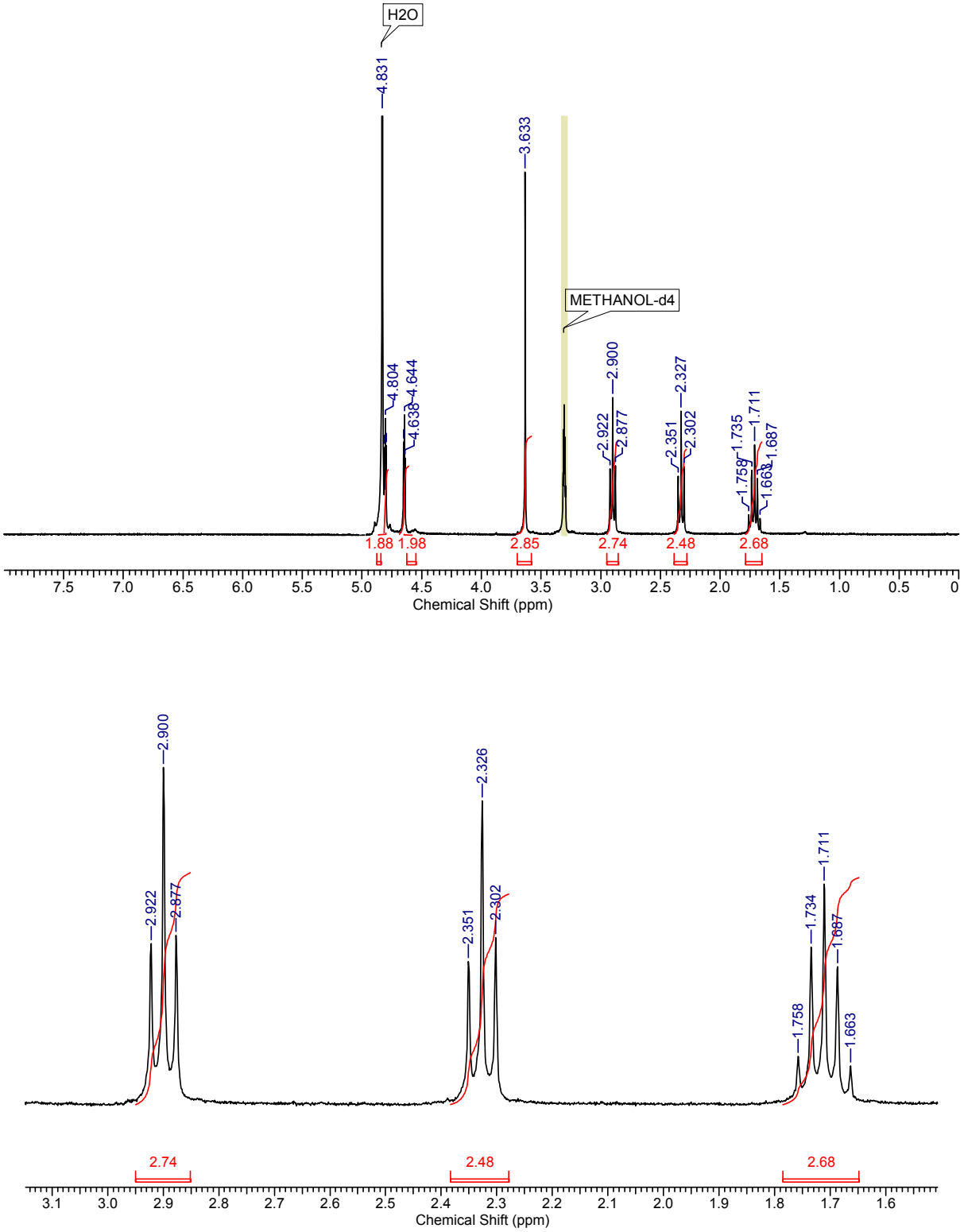

Figure S22 ^{1}H-NMR of **13** (300 MHz, CD_3OD)

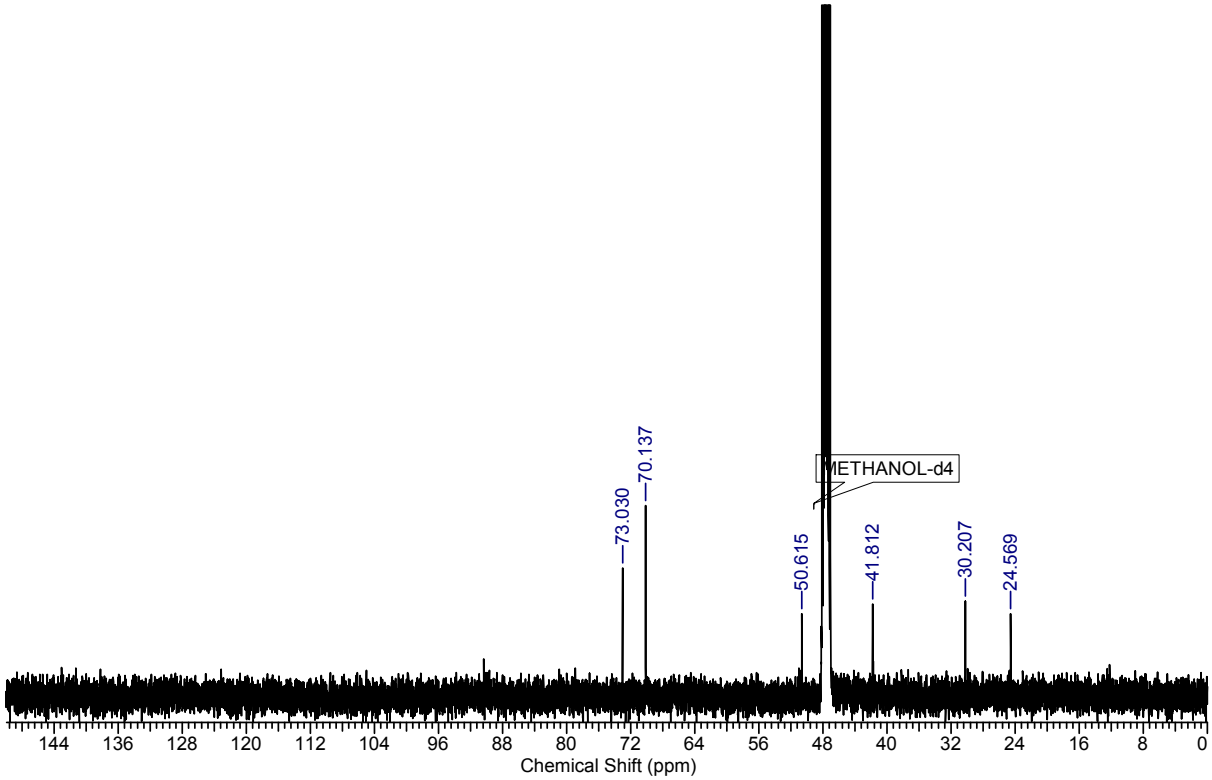

Figure S23 ^{13}C-NMR of **13** (500 MHz, CD_3OD)

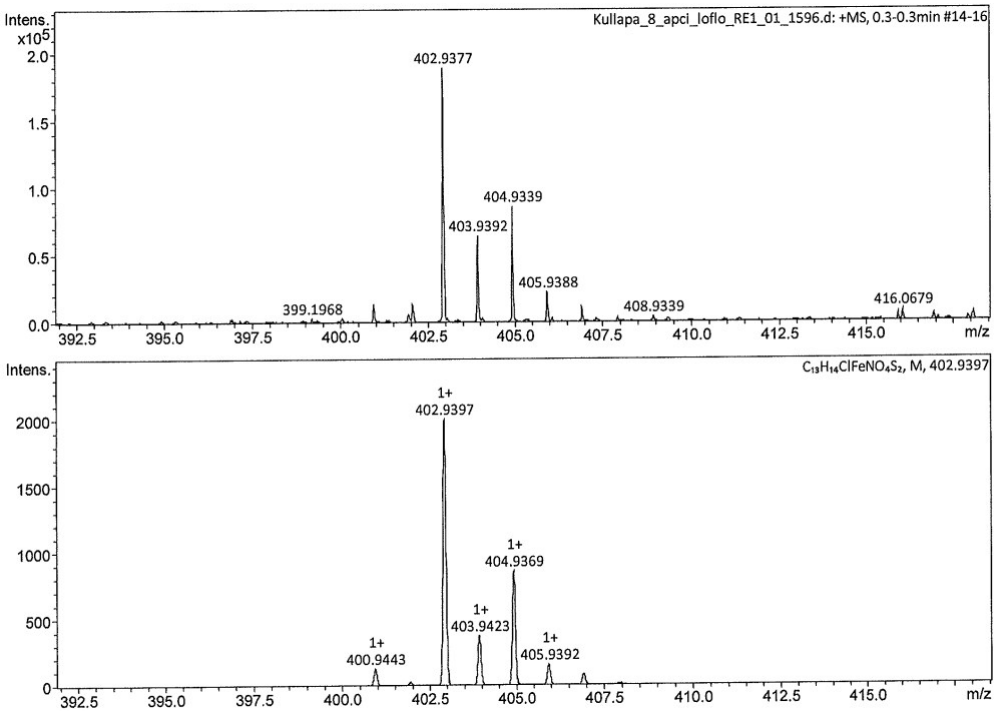

Figure S24 HRMS ESI of **4** (top: measured, bottom: calculated)

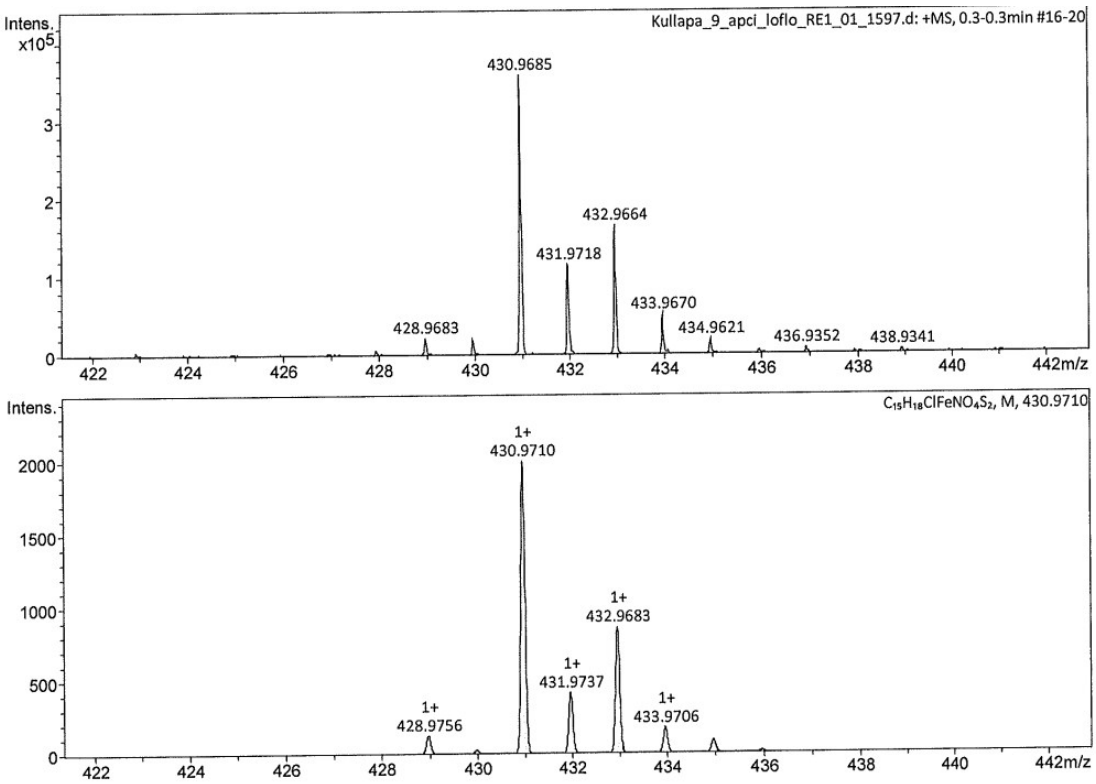

Figure S25 HRMS ESI of **5** (top: measured, bottom: calculated)

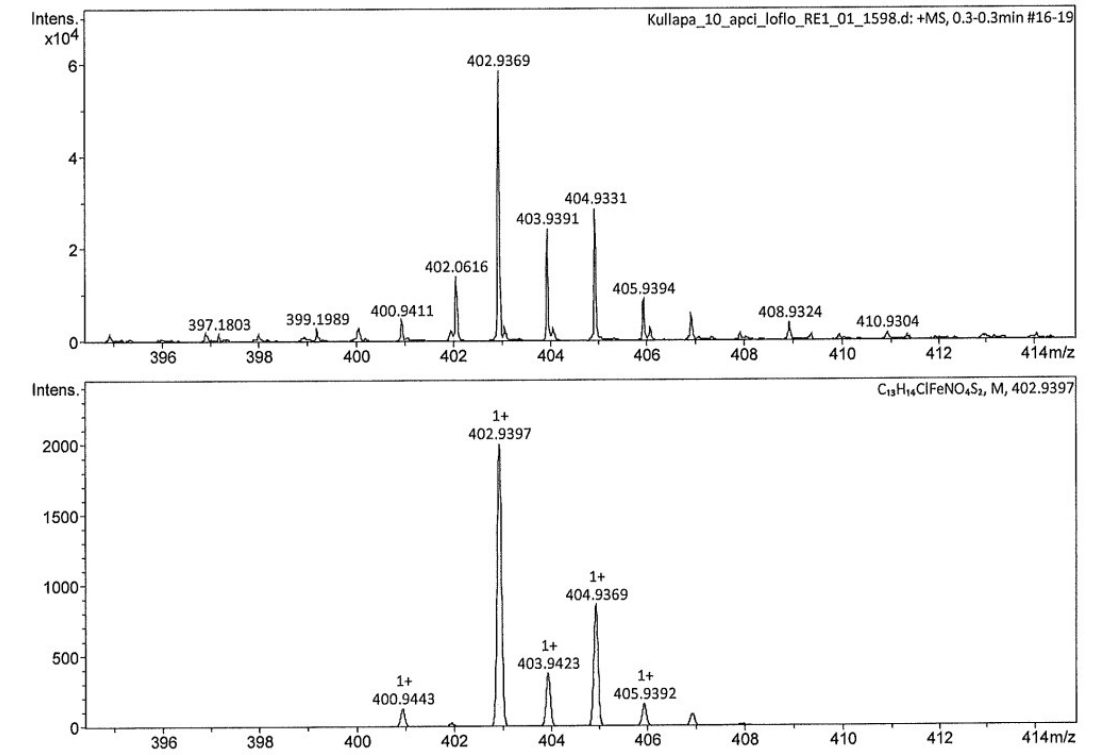

Figure S26 HRMS ESI of **6** (top: measured, bottom: calculated)

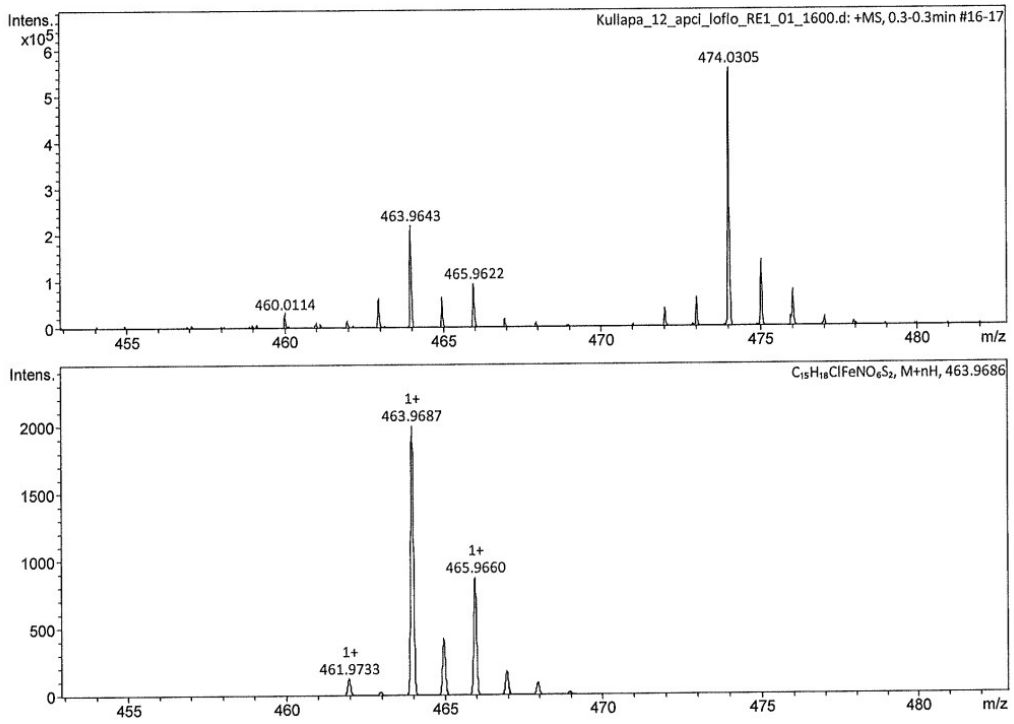

Figure S27 HRMS ESI of **7** (top: measured, bottom: calculated)

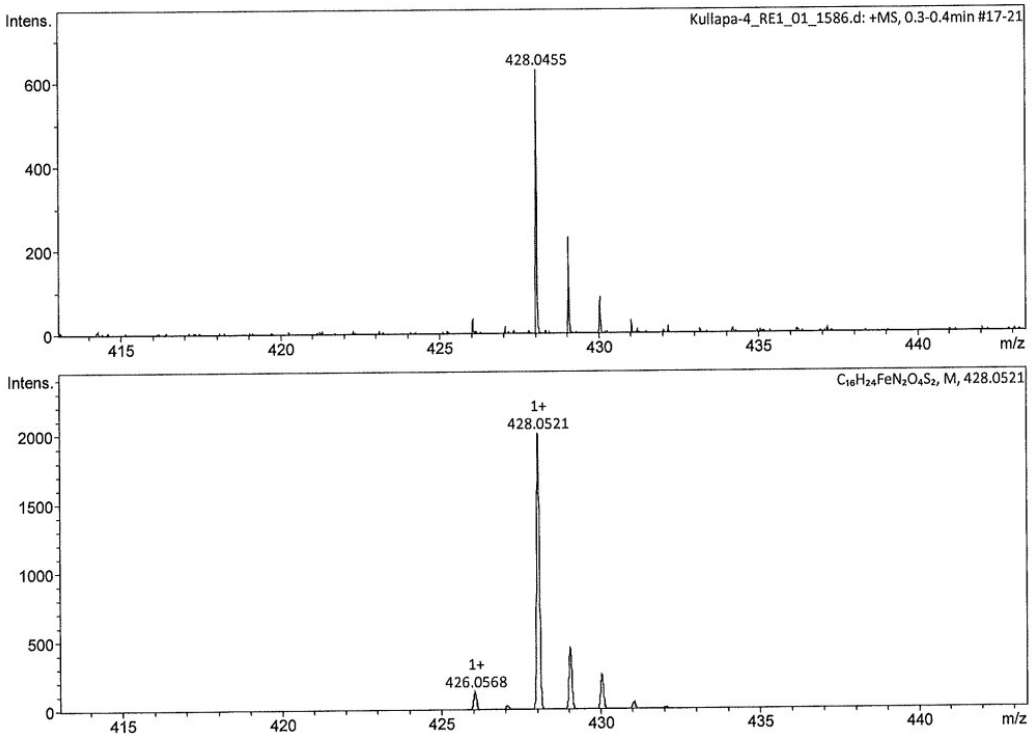

Figure S28 HRMS ESI of **8** (top: measured, bottom: calculated)

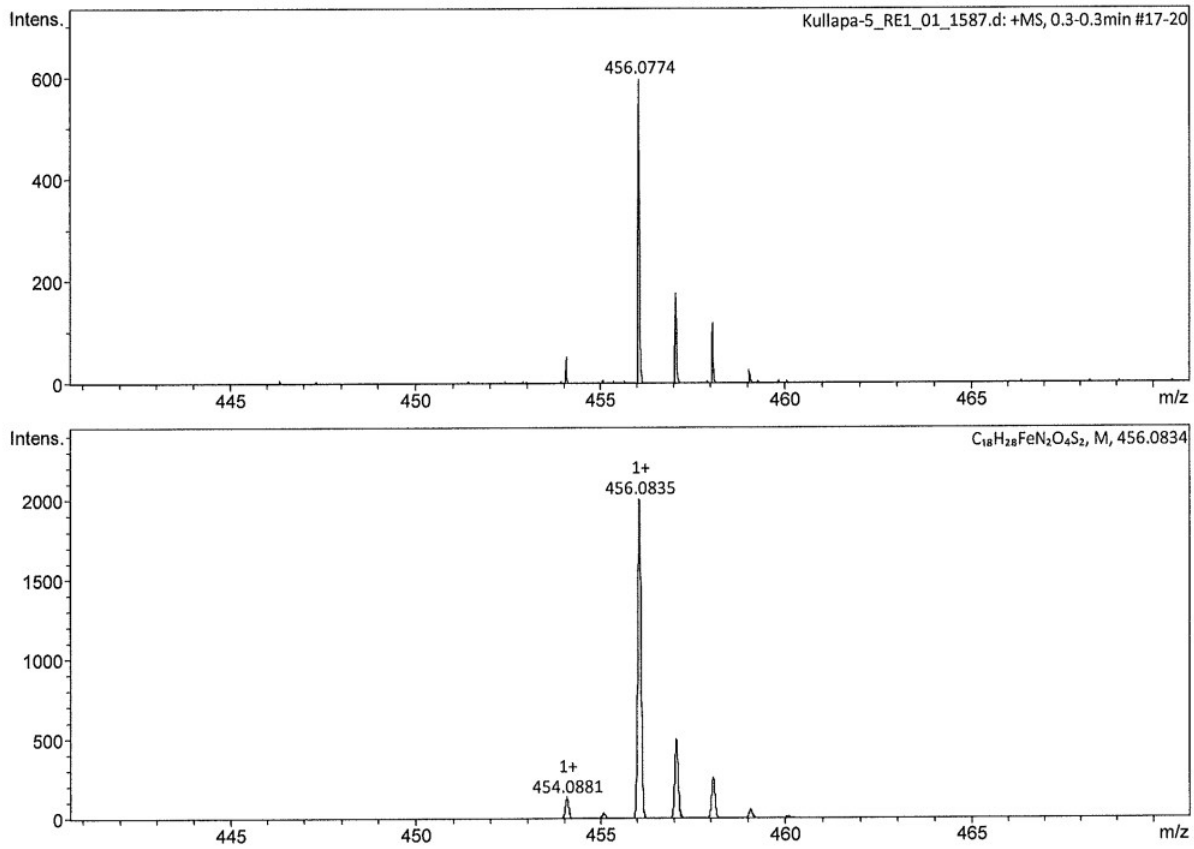

Figure S29 HRMS ESI of **9** (top: measured, bottom: calculated)

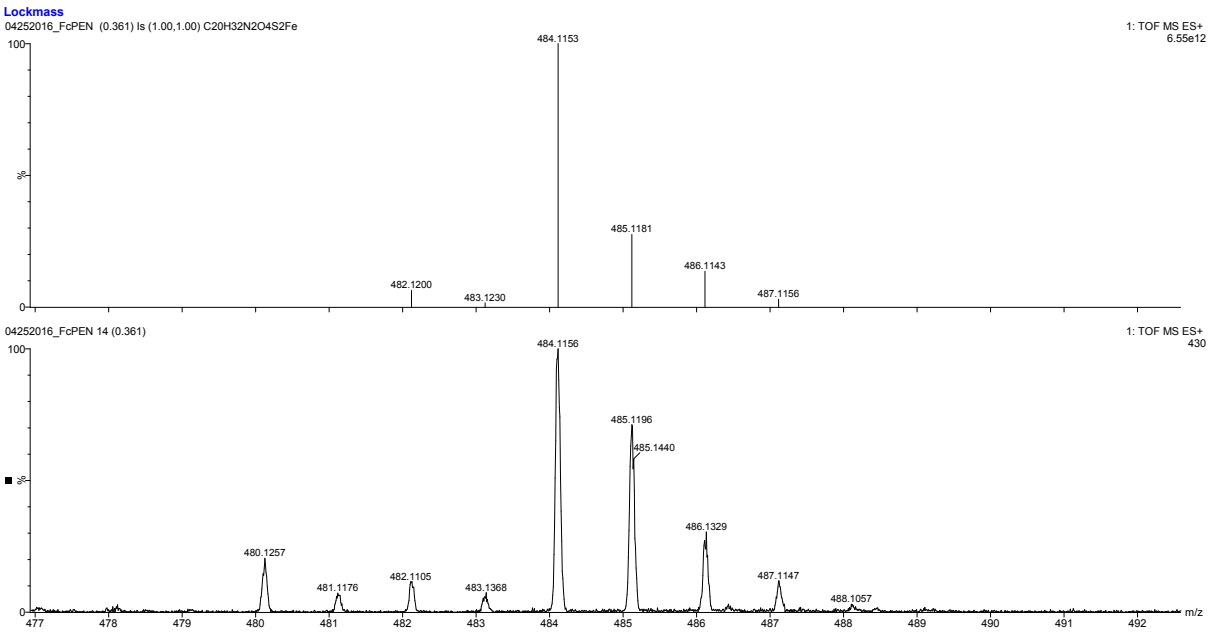

Figure S30 HRMS ESI of **10** (top: calculated, bottom: measured)

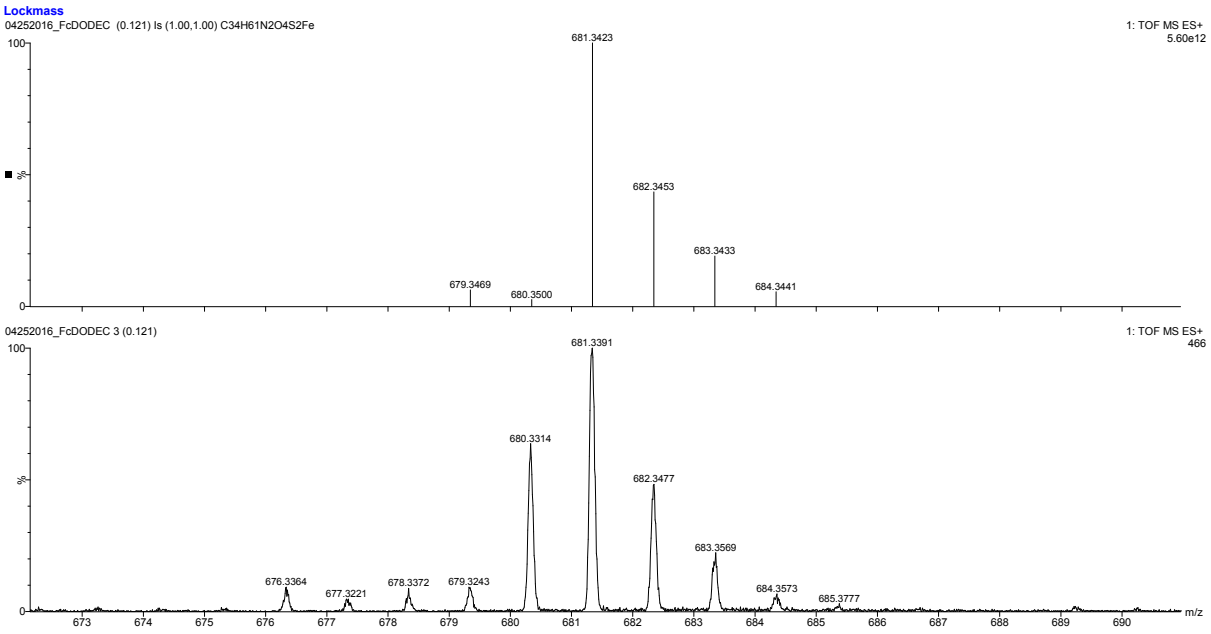

Figure S31 HRMS ESI of **11** (top: calculated, bottom: measured)

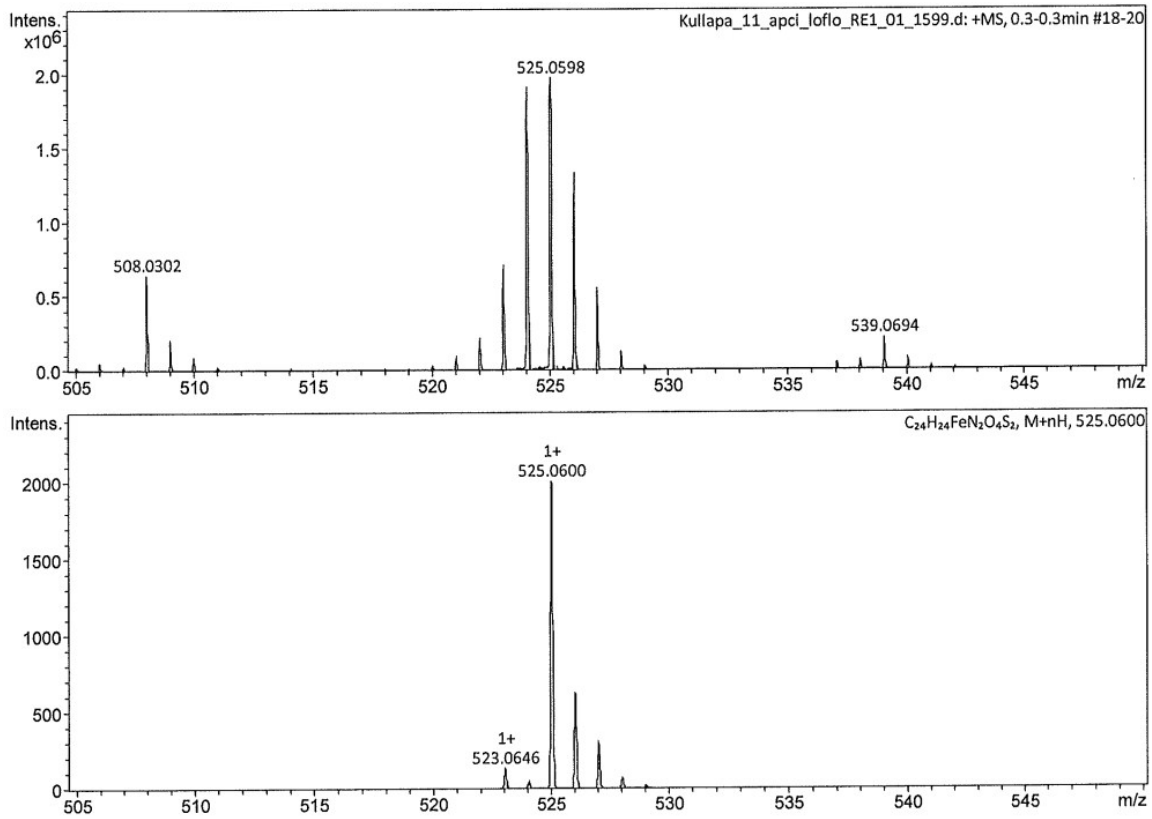

Figure S32 HRMS ESI of **12** (top: measured, bottom: calculated)

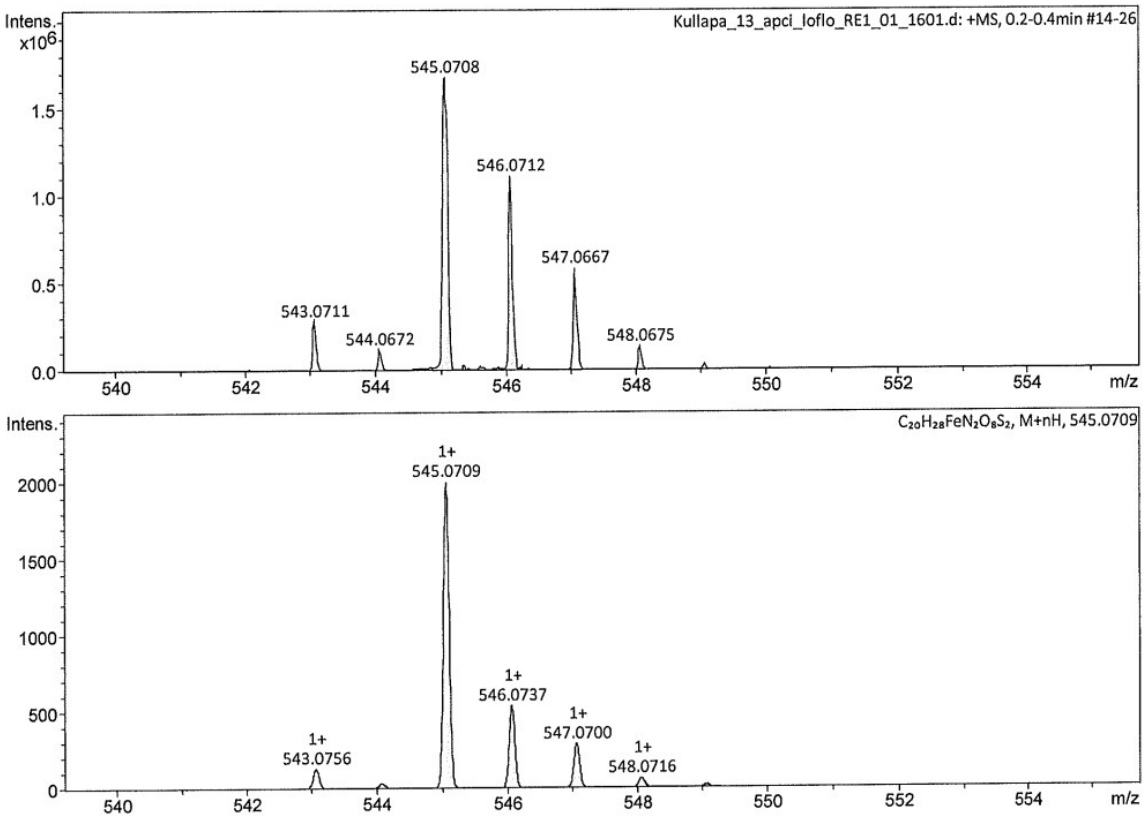

Figure S33 HRMS ESI of **13** (top: measured, bottom: calculated)

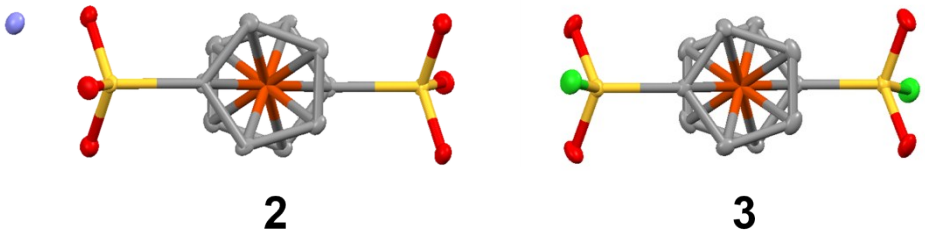

Figure S34 Ferrocene geometries of **2** and **3**

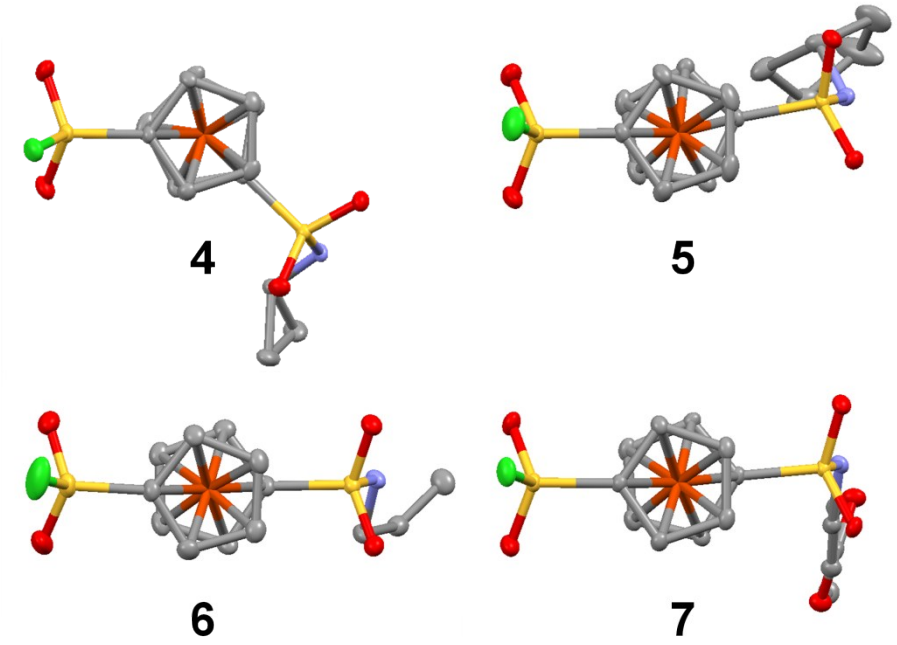

Figure S35 Ferrocene geometries of mono sulfonamides **4-7**

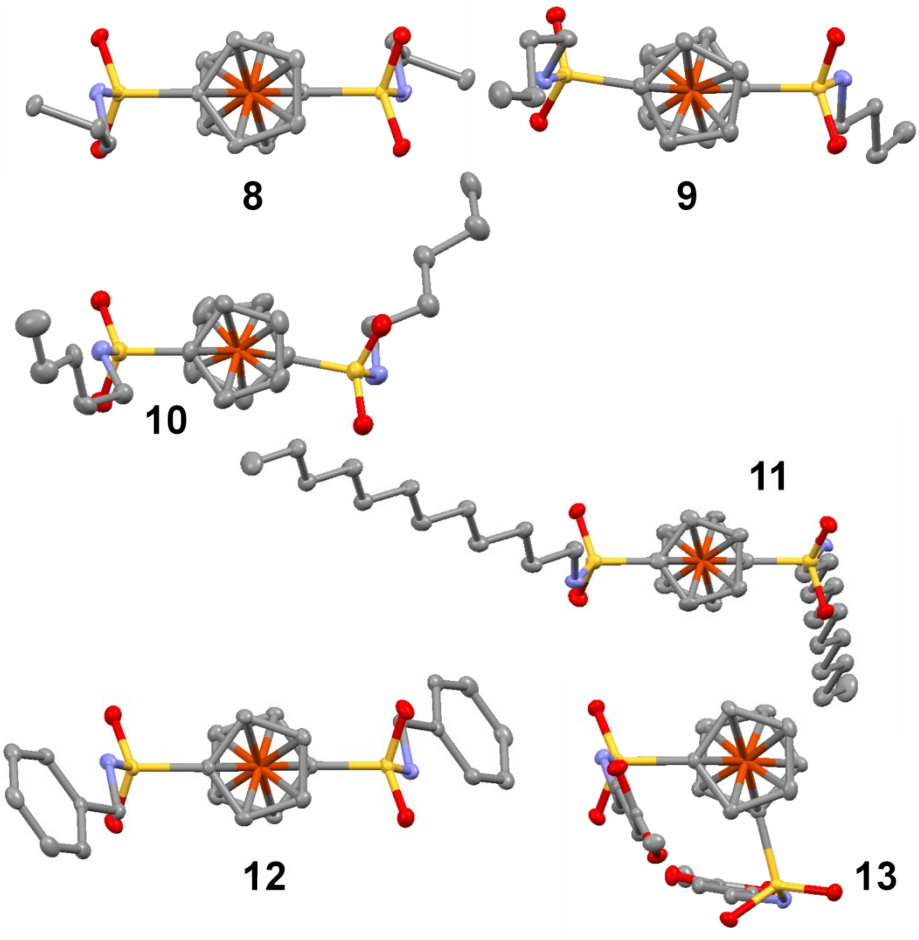

Figure S36 Ferrocene geometries of bis sulfonamides **8-13**

Table S1 Crystal data and refinement parameters of compounds **2-13**

Compound	**2**	**3**	**4**	**5**	**6**	**7**	**8**	**9**	**10**	**11**	**12**	**13**
Emp. form	$C_{10}H_{16}FeN_2O_6S_2$	$C_{10}H_8Cl_2FeO_4S_2$	$C_{13}H_{14}ClFeNO_4S_2$	$C_{15}H_{18}ClFeNO_4S_2$	$C_{13}H_{14}ClFeNO_4S_2$	$C_{15}H_{18}ClFeNO_6S_2$	$C_{16}H_{24}FeN_2O_4S_2$	$C_{18}H_{28}FeN_2O_4S_2$	$C_{20}H_{32}FeN_2O_4S_2$	$C_{34}H_{60}FeN_2O_4S_2$	$C_{24}H_{24}FeN_2O_4S_2$	$C_{20}H_{28}FeN_2O_8S_2$
Form. weight	380.22	383.03	403.67	431.72	403.67	463.72	428.34	456.40	484.45	680.83	524.42	544.41
Crystal system	Monoclinic	Monoclinic	Monoclinic	Triclinic	Triclinic	Triclinic	Monoclinic	Monoclinic	Triclinic	Monoclinic	Monoclinic	Monoclinic
Space group	$P2_1/c$	$P2_1/c$	$P2_1/n$	P-1	P-1	P-1	$P2_1/c$	$P2_1/c$	P-1	$P2_1/c$	$P2_1/n$	C2/c
a/ Å	9.8760(6)	7.9181(3)	14.2039(16)	7.6445(2)	7.4865(3)	6.1935(2)	9.1202(5)	8.8433(2)	11.6821(12)	9.8354(18)	8.5381(3)	29.718(3)
b/ Å	5.5764(3)	7.7541(2)	6.7783(8)	10.0532(2)	7.5363(3)	6.8408(3)	12.7387(6)	23.1800(5)	12.4196(13)	7.6469(14)	9.4320(4)	6.7980(7)
c/ Å	12.5720(7)	10.7240(4)	16.7399(19)	12.1654(3)	14.9763(6)	21.6753(8)	8.0686(4)	10.4639(2)	15.6230(16)	46.916(9)	13.8114(5)	11.6656(12)
α(°)	90	90	90	68.8020(10)	87.392(2)	90.4550(10)	90	90	99.412(7)	90	90	90
β(°)	101.134(3)	99.0150(10)	106.824(5)	87.4870(10)	86.354(2)	93.3320(10)	111.388(2)	108.4280(10)	94.062(7)	90.805(11)	95.640(2)	111.369(7)
γ(°)	90	90	90	84.9240(10)	65.8810(10)	108.2330(10)	90	90	94.877(7)	90	90	90
Volume ($Å^3$)	679.34(7)	650.30(4)	1542.7(3)	868.18(4)	769.47(5)	870.44(6)	872.85(8)	2034.98(8)	2219.8(4)	3528.2(11)	1106.87(7)	2194.7(4)
Z	2	2	4	2	2	2	2	4	4	4	2	4
Dc (Mg/m^3)	1.859	1.956	1.738	1.651	1.742	1.769	1.630	1.493	1.450	1.285	1.573	1.654
μ (mm^{-1})	1.446	1.895	1.436	1.282	12.150	1.294	1.128	0.973	0.896	0.584	0.906	0.930
F(000)	392	384	824	444	412	476	448	964	900	1480	544	1144
Reflections collected	1212	4439	92930	12452	8179	23712	6294	29964	23581	124602	15774	15126
Data/Restraints/Parameters	1212 / 1 / 113	1147 / 0 / 88	3110 / 0 / 199	3770 / 0 / 217	2329 / 0 / 208	3795 / 0 / 236	1908 / 0 / 116	4436 / 0 / 246	9199 / 0 / 527	7438 / 0 / 390	2411 / 0 / 151	2393 / 0 / 151
GOF on F^2	1.224	1.169	1.125	1.055	1.069	0.965	1.366	1.076	1.200	1.071	0.959	1.026
R1 (on F_o^2, $I > 2\sigma(I)$)	0.0571	0.0223	0.0383	0.0301	0.0328	0.0335	0.0394	0.0355	0.0775	0.1036	0.0299	0.0305
wR2 (on F_o^2, $I > 2\sigma(I)$)	0.1645	0.0612	0.0819	0.0747	0.0913	0.0814	0.1122	0.1011	0.2039	0.2527	0.0757	0.0807
R1 (all data)	0.0759	0.0228	0.0396	0.0308	0.0335	0.0363	0.0405	0.0387	0.1079	0.1584	0.0304	0.0317
wR2 (all data)	0.1743	0.0620	0.0825	0.0754	0.0921	0.0846	0.1133	0.1048	0.2221	0.2955	0.0765	0.0816

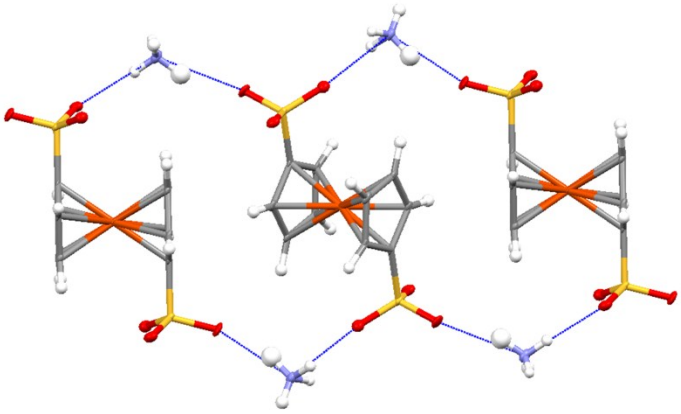

2

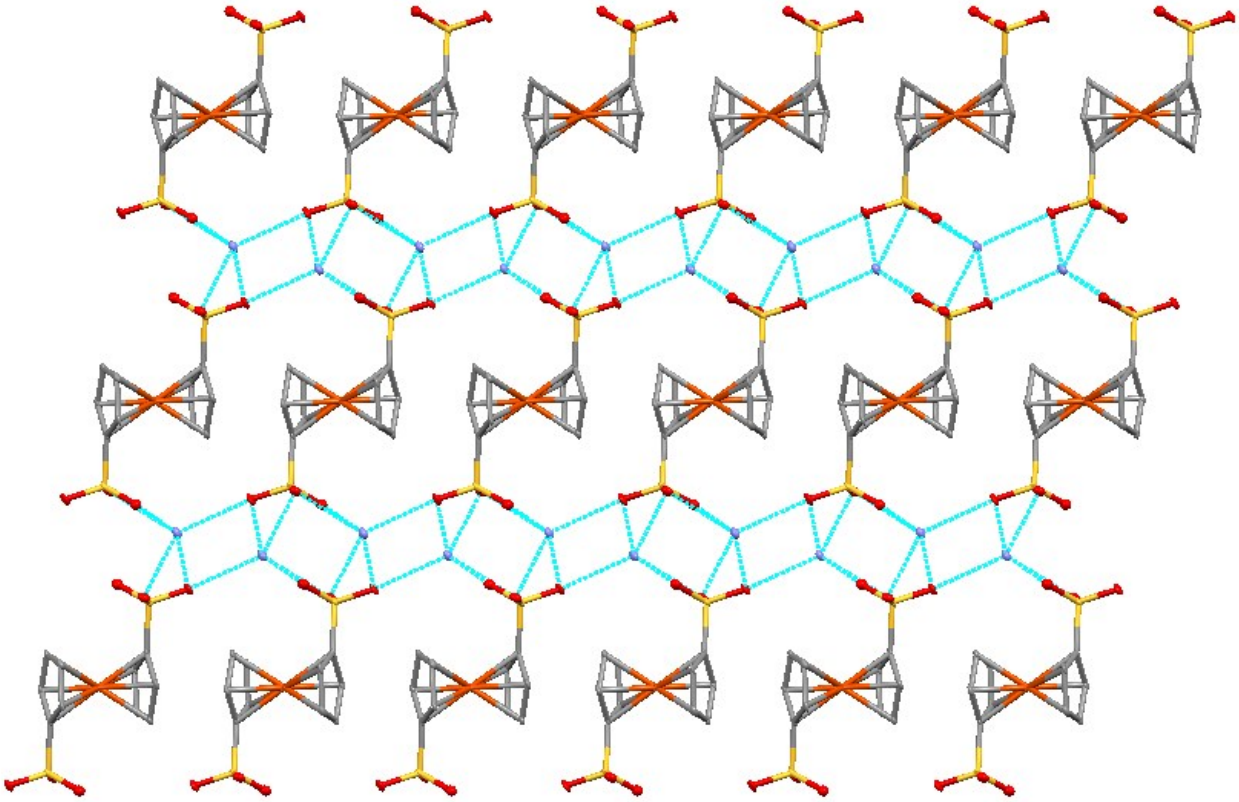

Figure S37 The packing diagrams with intermolecular hydrogen bonding interactions (blue dash lines) of **2**

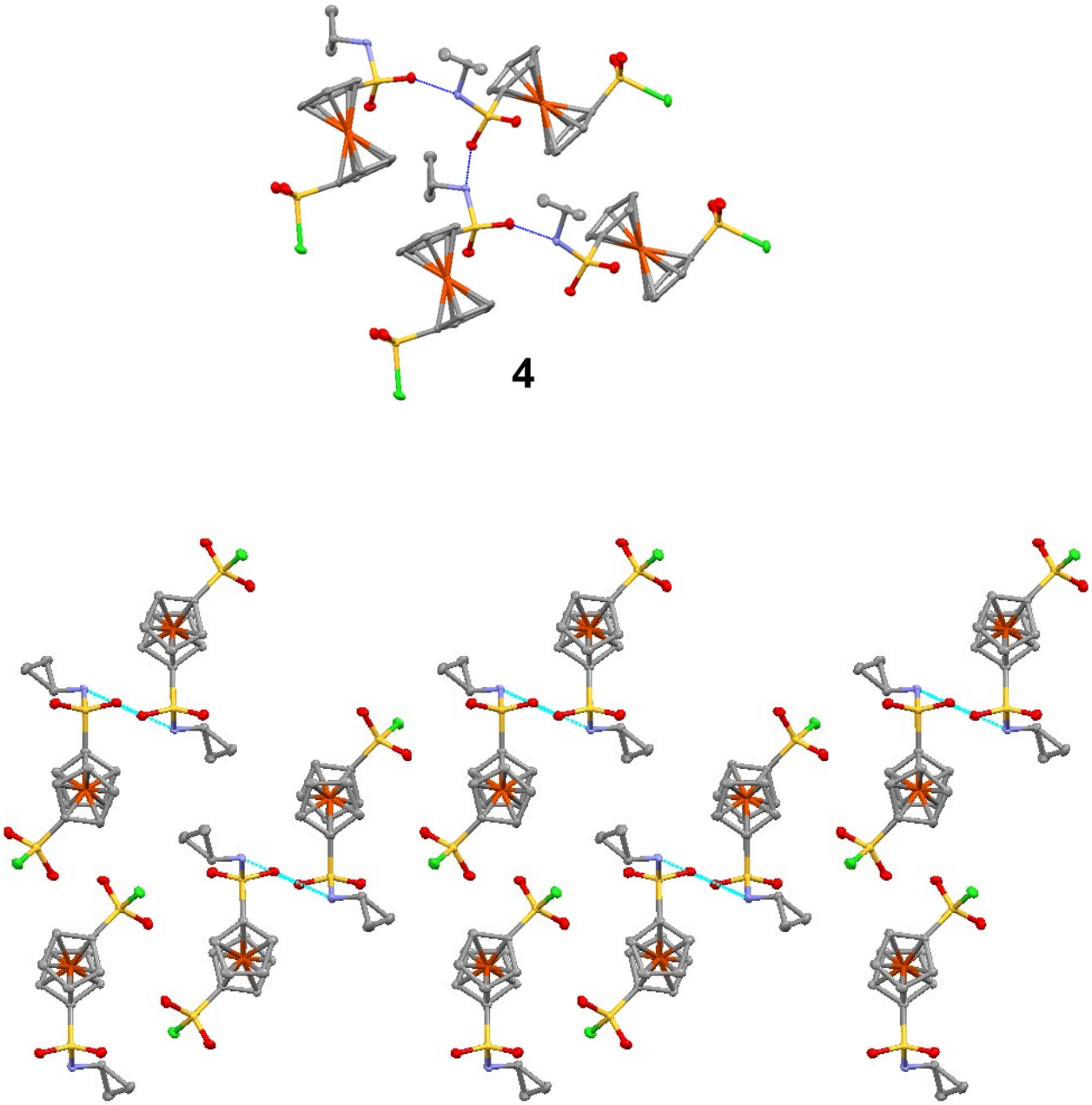

Figure S38 The packing diagrams with intermolecular hydrogen bonding interactions (blue dash lines) of **4**

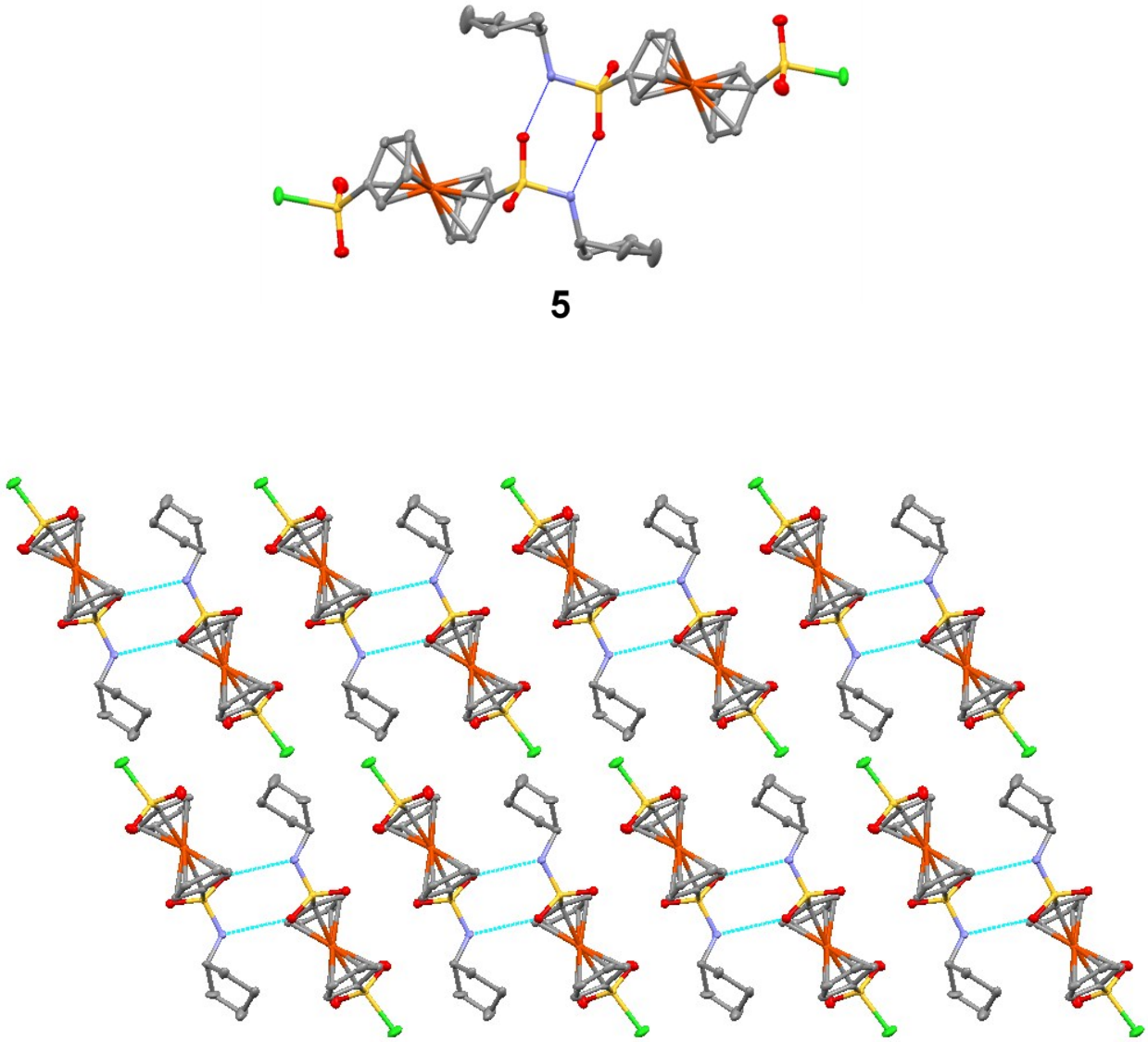

Figure S39 The packing diagrams with intermolecular hydrogen bonding interactions (blue dash lines) of **5**

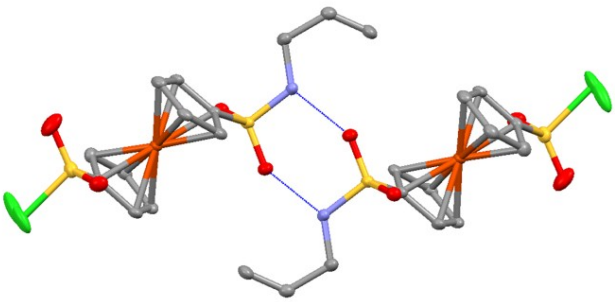

6

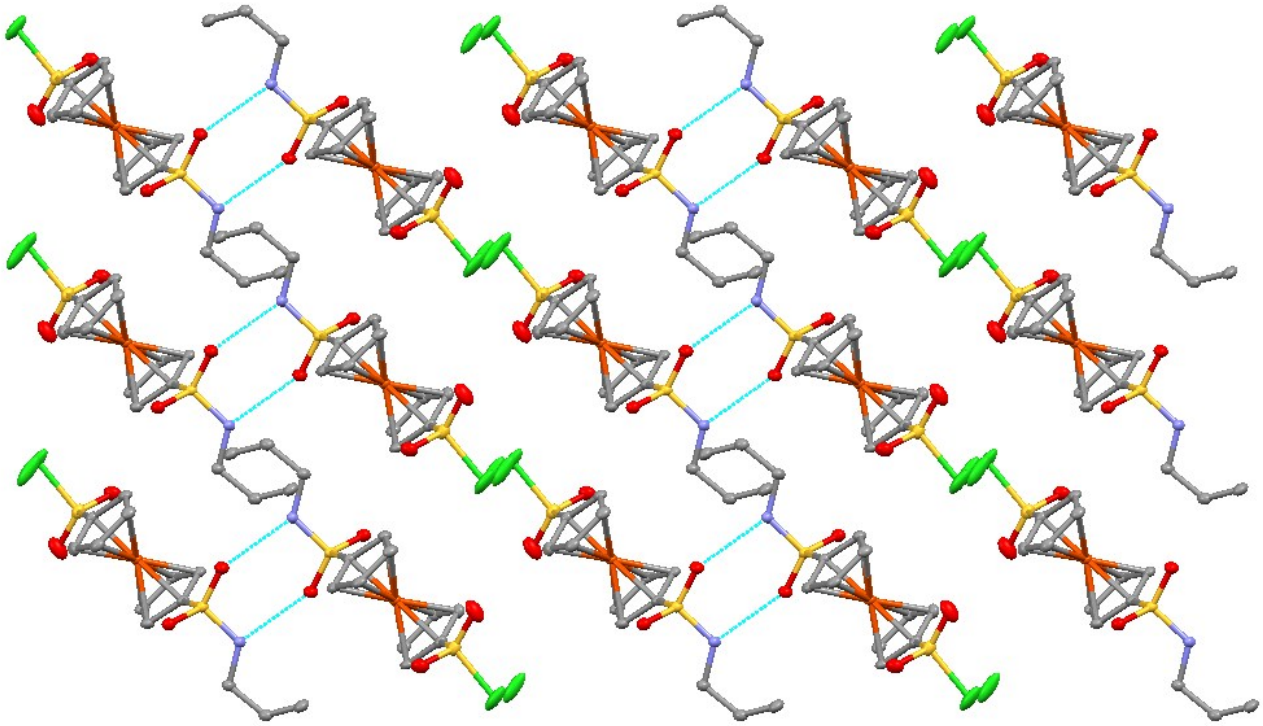

Figure S40 The packing diagrams with intermolecular hydrogen bonding interactions (blue dash lines) of **6**

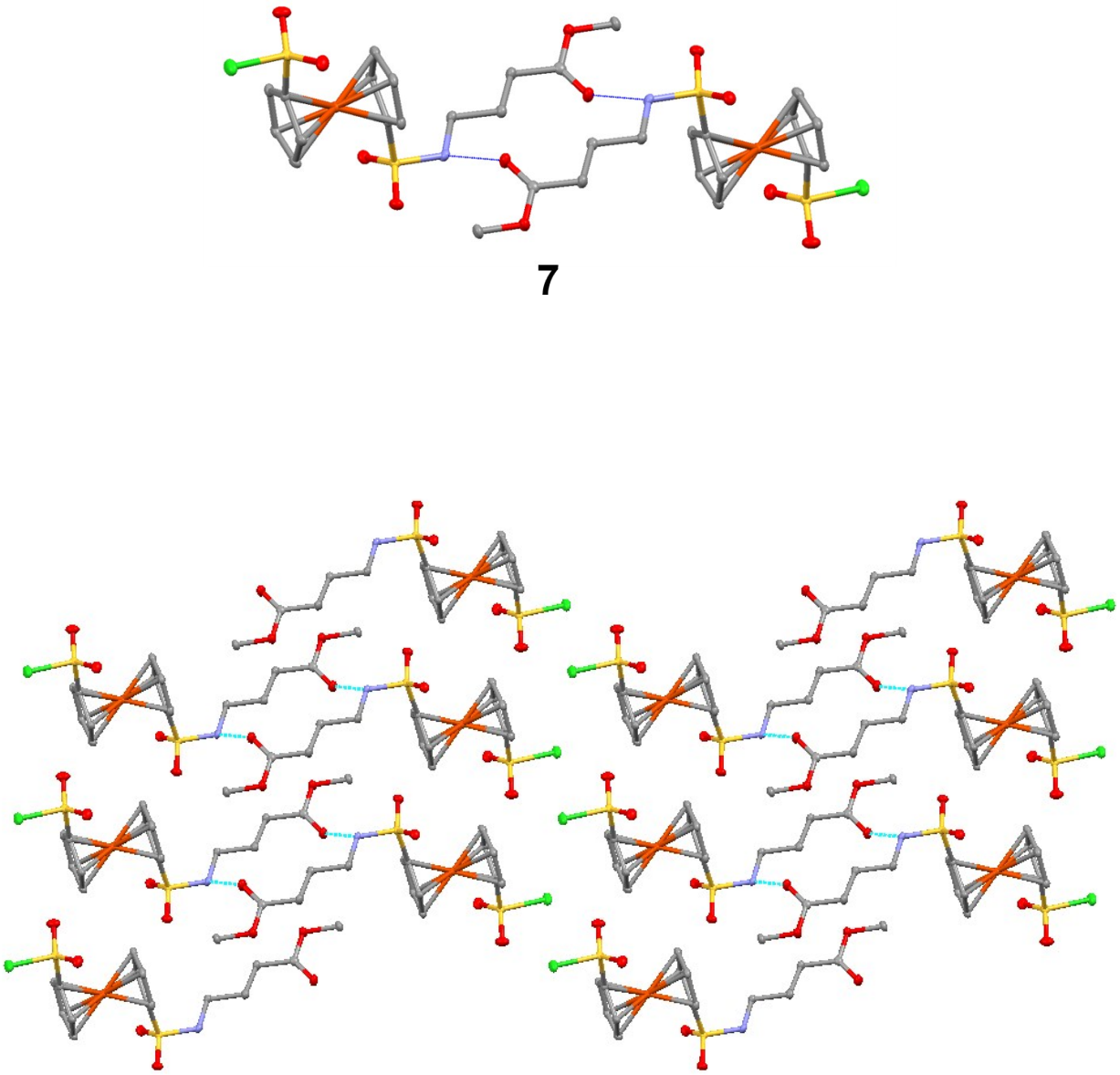

Figure S41 The packing diagrams with intermolecular hydrogen bonding interactions (blue dash lines) of **7**

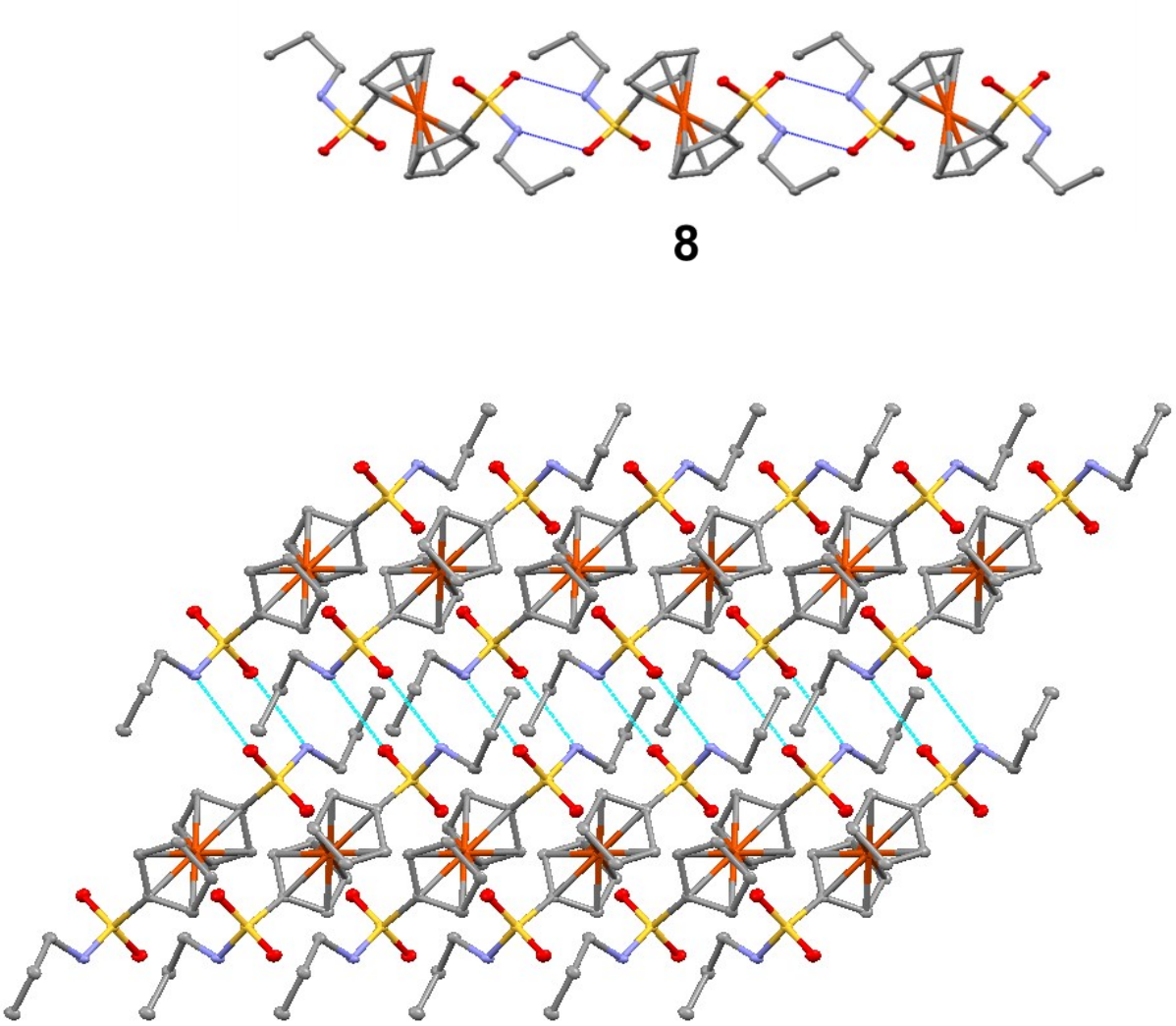

Figure S42 The packing diagrams with intermolecular hydrogen bonding interactions (blue dash lines) of **8**

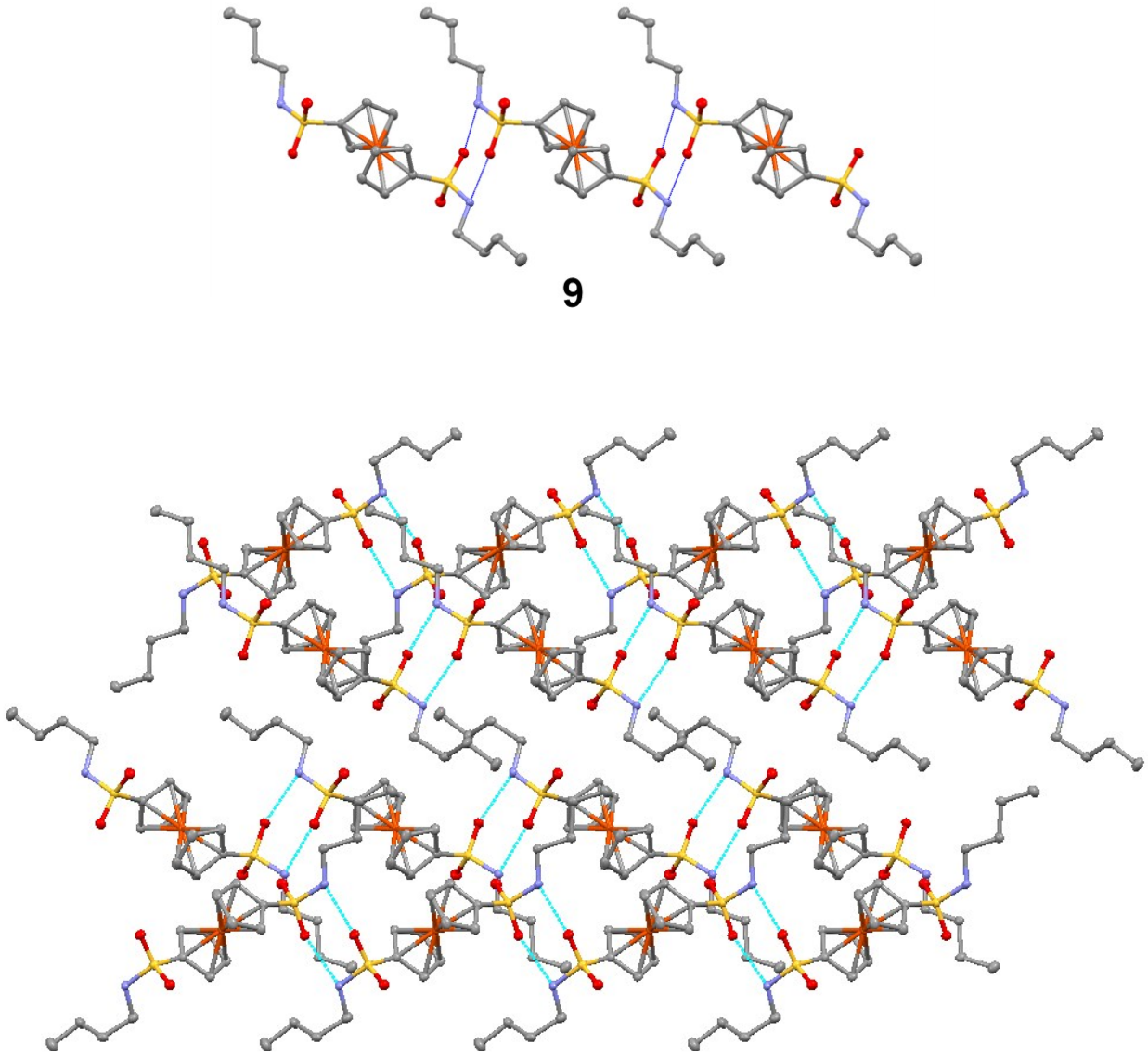

Figure S43 The packing diagrams with intermolecular hydrogen bonding interactions (blue dash lines) of **9**

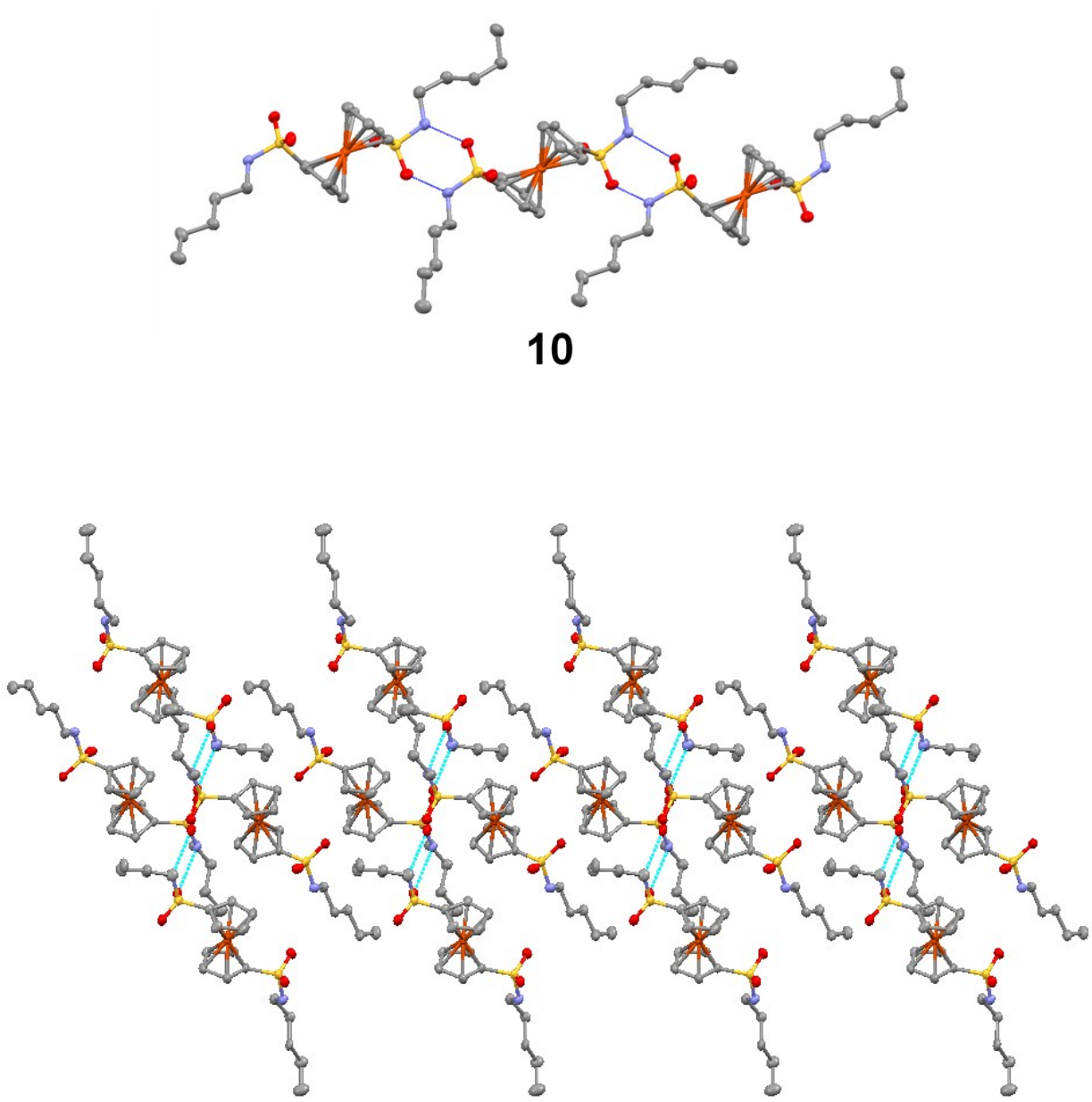

Figure S44 The packing diagrams with intermolecular hydrogen bonding interactions (blue dash lines) of **10**

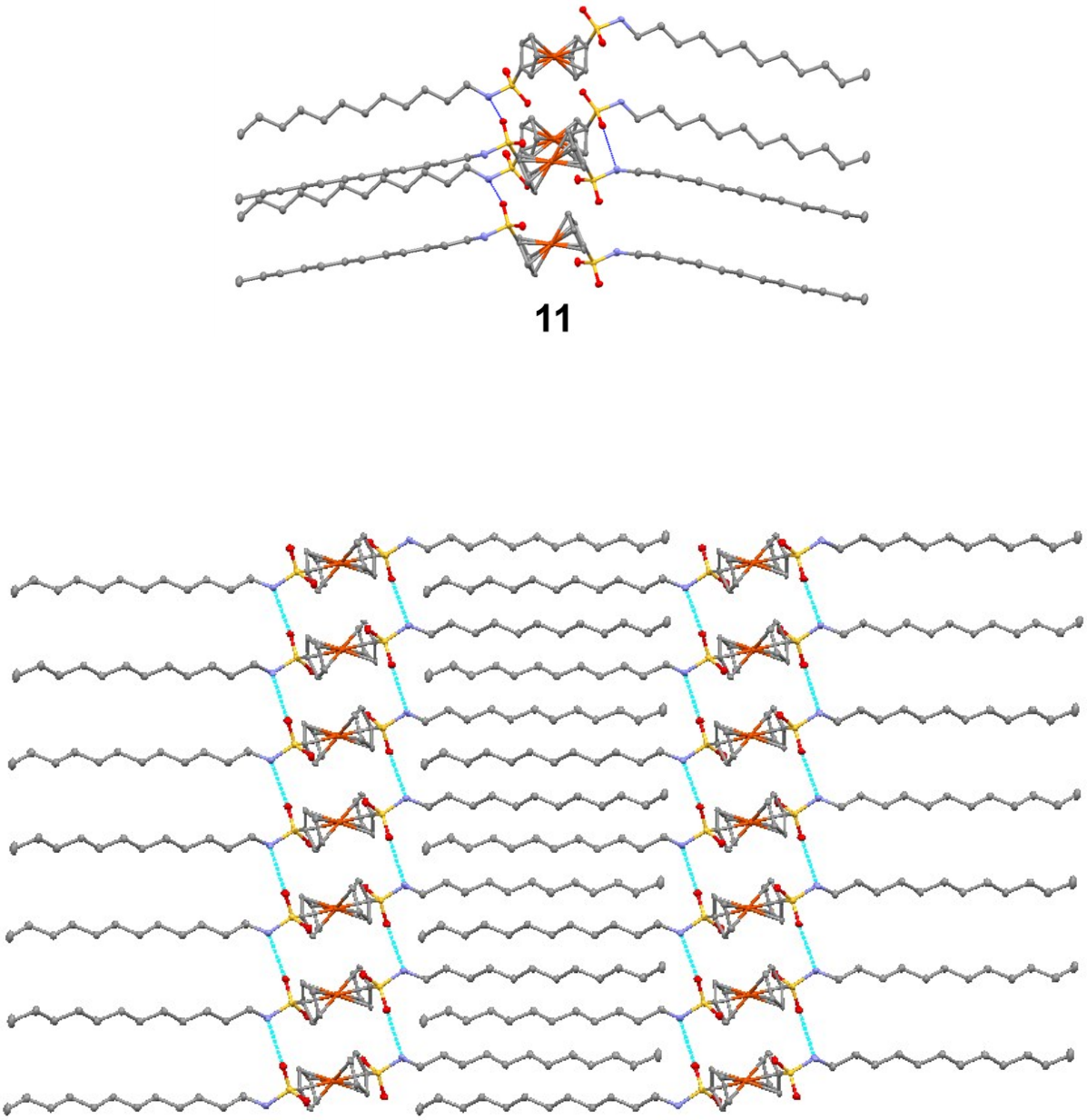

Figure S45 The packing diagrams with intermolecular hydrogen bonding interactions (blue dash lines) of **11**

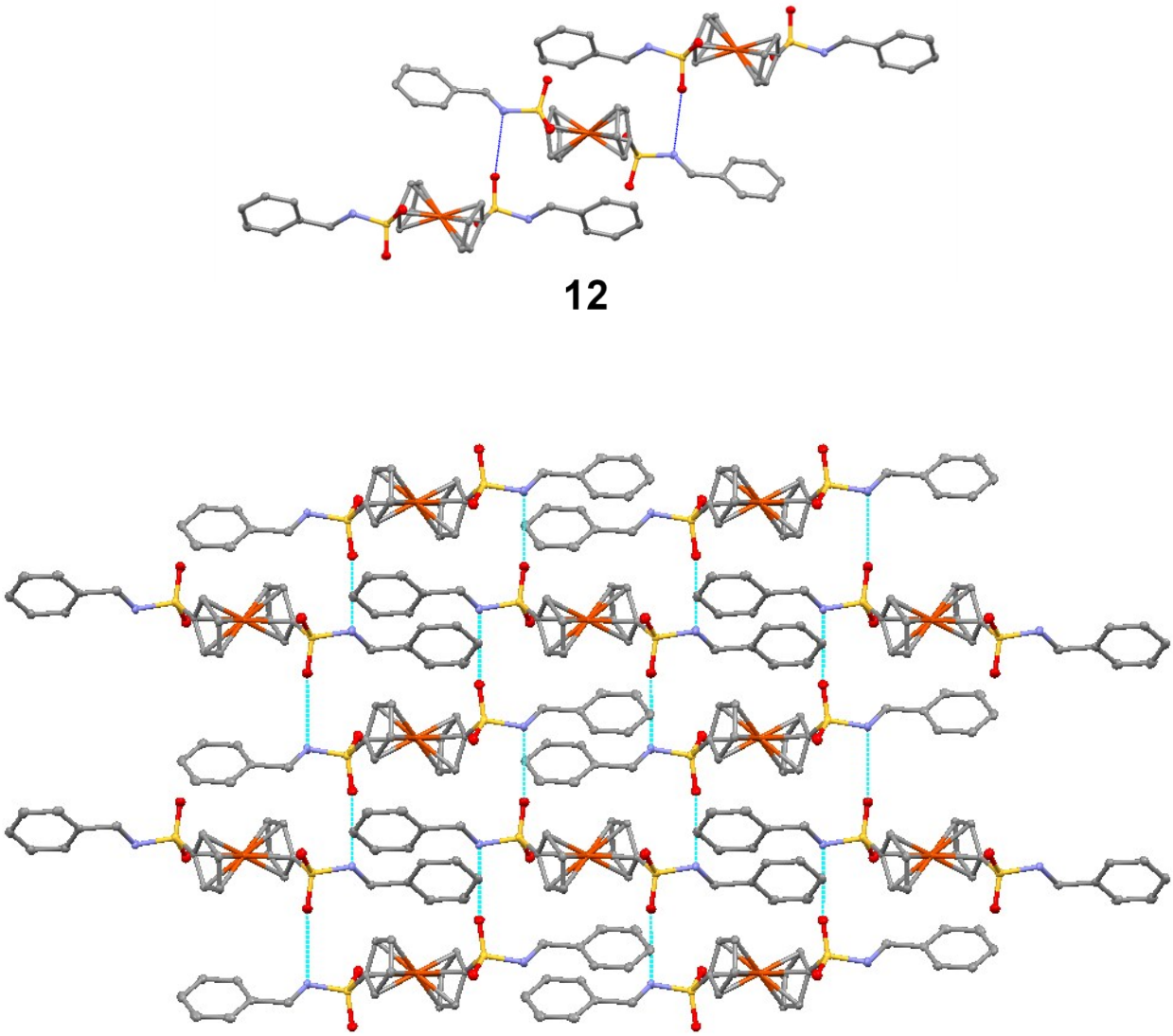

Figure S46 The packing diagrams with intermolecular hydrogen bonding interactions (blue dash lines) of **12**

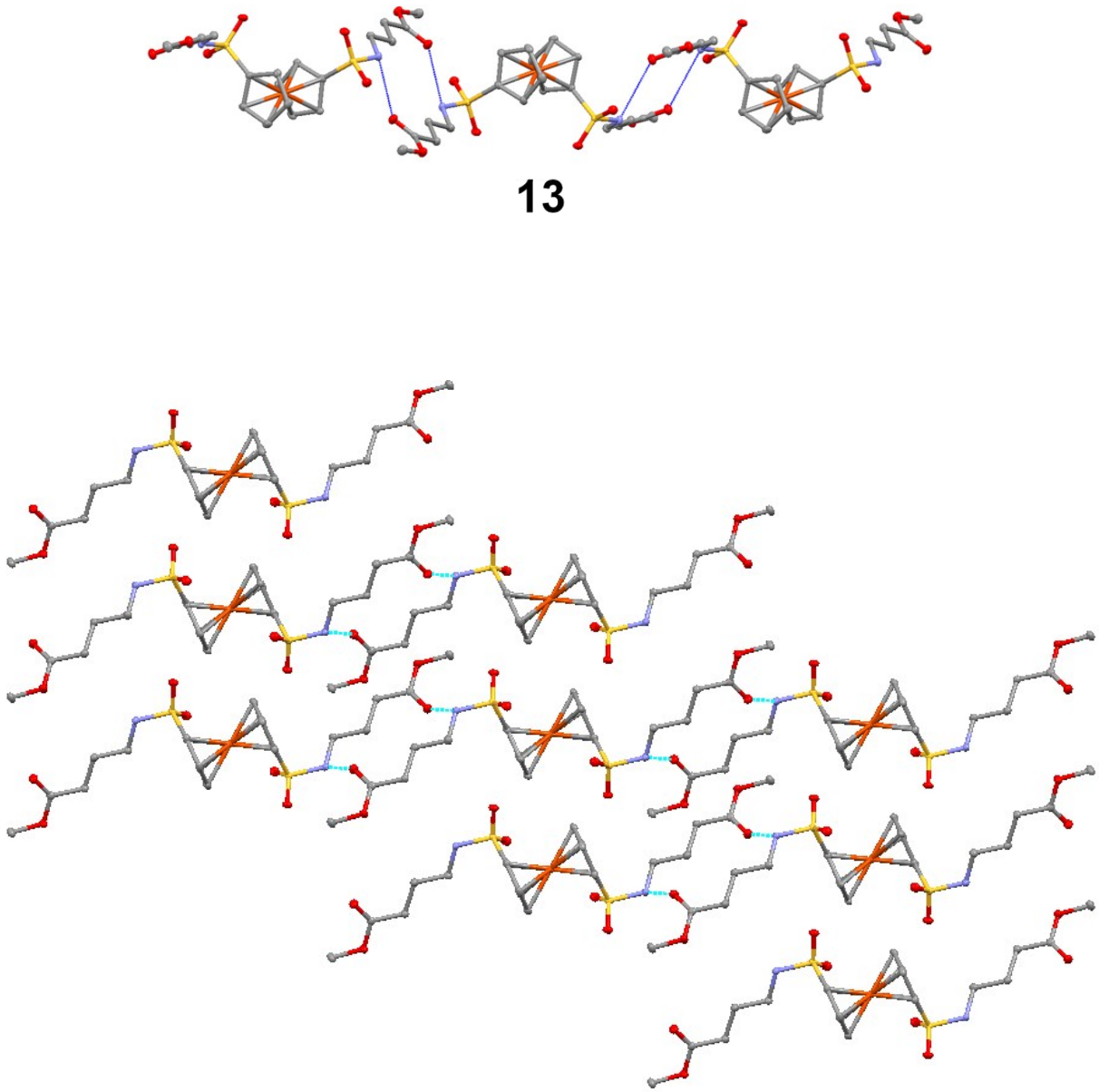

Figure S47 The packing diagrams with intermolecular hydrogen bonding interactions (blue dash lines) of **13**

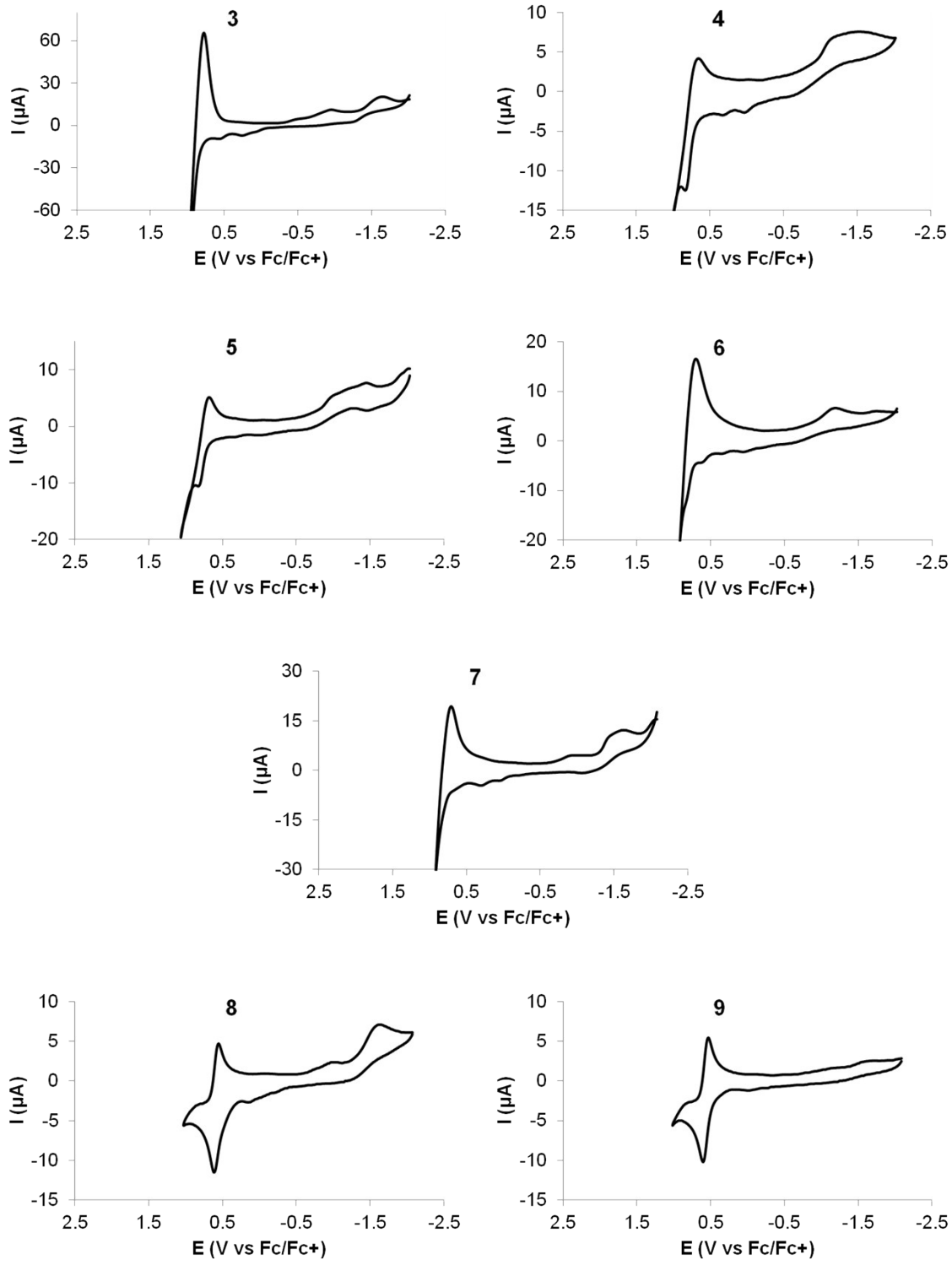
3
I (µA)
E (V vs Fc/Fc+)
4
I (µA)
E (V vs Fc/Fc+)
5
I (µA)
E (V vs Fc/Fc+)
6
I (µA)
E (V vs Fc/Fc+)
7
I (µA)
E (V vs Fc/Fc+)
8
I (µA)
E (V vs Fc/Fc+)
9
I (µA)
E (V vs Fc/Fc+)

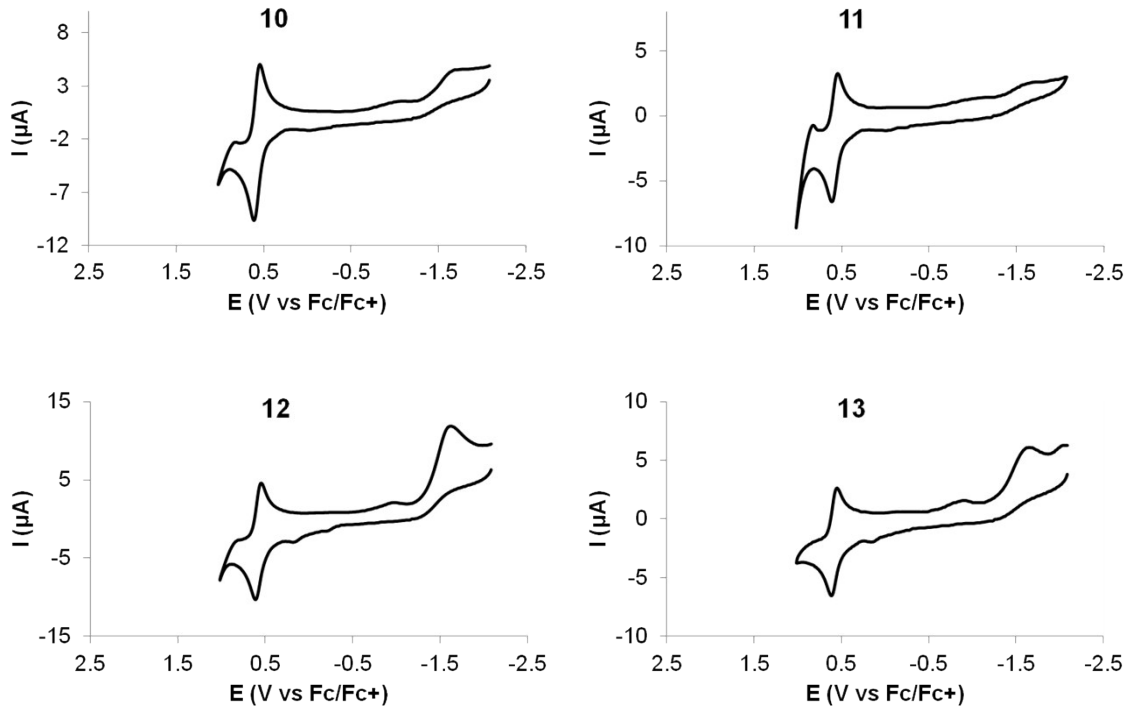

Figure S48 Cyclic voltammograms of compounds **3-13** (10^{-3} M) in acetonitrile/0.1 M tetra-n-butylammonium hexafluorophosphate ($TBAPF_6$)

Table S2 Electrochemical data for compounds **3-13**

compound	E_{pc} (V)	E_{pa} (V)	$E^{o'}$ (V)	compound	E_{pc} (V)	E_{pa} (V)	$E^{o'}$ (V)
3	0.798	-	-	**8**	0.573	0.591	0.582
4	0.697	-	-	**9**	0.541	0.587	0.564
5	0.689	-	-	**10**	0.545	0.591	0.568
6	0.710	-	-	**11**	0.569	0.623	0.596
7	0.711	-	-	**12**	0.551	0.625	0.588
				13	0.554	0.582	0.568

Cyclic voltammograms were obtained at 298 K using a standard three electrode cell and electrochemical analyzer BAS 100B from Bioanalytical systems. The sample concentration were 10^{-3} M in acetronitrile (ACN) in the presence of 0.1 M tetra-n-butylammonium hexafluorophosphate ($TBAPF_6$) as a supporting electrolyte. A gold working electrode (planar circular area 0.79 mm^2), a silver wire pseudo-reference electrode, a platinum wire auxiliary electrode, and ferrocene internal

standard were used in the measurement. The working electrode was polished with 0.05 μm alumina on a polish pad. The electrode was rinsed with ethanol after each polishing and dried with a Kimwipe. The scan rate for all measurement was 100 mV/s. Approximated formal potentials for a reversible redox couples ($E^{o'} = [E_{pc} + E_{pa}]/2$), and E_{pc} in case of irreversible process, were all referenced against ferrocene/ferrocenium couple (Fc/Fc^{+}).[1]

Reference

1. R. R. Gagné, C. A. Koval, and G. C. Lisensky, *Inorg. Chem.*, 1980, 19, 2854-2855.